INVESTIGATION OF KAOLIN IN EASTERN REDWOOD COUNTY, MINNESOTA, USING GRAVITY, MAGNETIC, AND ELECTRICAL RESISTIVITY METHODS

by
Val W. Chandler*, S. Hauck, M. Severson,
J. Heine, J. Reichhoff, and Bryan D. Schaap*

October 1990

Technical Report
NRRI/GMIN-TR-89-14

Natural Resources Research Institute
University of Minnesota, Duluth
5013 Miller Trunk Highway
Duluth, Minnesota 55811

*Minnesota Geological Survey
University of Minnesota
2642 University Avenue
St. Paul, Minnesota 55114-1057

ABSTRACT

The utility of gravity, magnetic and electrical resistivity methods for kaolin exploration was evaluated on a test-drilled 300-meter by 600-meter prospect in the Minnesota River Valley in eastern Redwood County, Minnesota. Seven Wenner soundings and three resistivity profiles were taken over the prospect, and interpretations were constrained by direct determinations at nearby bedrock exposures and by drill hole (regolith) data. High-precision gravity data also appear to reflect thickness variations in the low-density kaolin. The magnetometer is not sensitive to the kaolin itself, but it may be useful in detecting rocks in the protolith that yield chlorite-rich, weathered clays, such as diabase dikes.

TABLE OF CONTENTS

LIST OF FIGURES

LIST OF PLATES

LIST OF TABLES

LIST OF APPENDICES

INTRODUCTION

The use of kaolin as a waste-reducing agent in the production of portland cement has led to renewed interest in the low-grade kaolin in the Minnesota River Valley in southwestern Minnesota. The use of geophysical methods to target drilling would greatly reduce the cost of exploration. In this study we investigated the effectiveness of gravity, magnetic, and electrical resistivity methods in the exploration of the kaolin deposits.

Physical Setting

The main survey area was a 300-meter by 600-meter prospect in the south-central part of Section 24, T. 112 N., R. 34 W., where kaolin underlies the floodplain of the Minnesota River. In this report, this area is referred to as the "beanfield" (Plate 1A). Five north-south lines were staked 200 feet (60.48 m) apart at 100-foot (30.48 m) intervals (Plate 1A). All numbering of the stakes was referenced to an east-west base line (position 0 on all lines) in the northern part of the study area that transected all lines. The UTM location and elevation of each stake were surveyed using rod and theodolite, and all surveying was tied to a benchmark on the Minnesota River bridge near the southwest corner of Section 12, T. 112 N., R. 34 W. The beanfield is characterized by generally low relief, although bedrock outcrops at the extreme northern end of the area form an east-west ridge 10 to 15 meters above the flood plain. The kaolin is not exposed in the beanfield, but seven recently drilled split-tube auger test holes (Plate 1A and Table 3) provided a means of evaluating the geophysical methods. None of these holes penetrated fresh rock,

but all except holes 1 and 3 intersected grus and thus provide a minimum depth for the bottom of the kaolin. The kaolin is covered by 1 to 3 meters of silty organic soil.

The second survey area lies about 3000 feet (0.91 km) from the beanfield, along the south wall of the Minnesota River Valley. In this report, this area is referred to as the "farmyard" (Plate 1B). The abandoned farmyard has grusy outcrops, and a freshly cut drill road going up the valley wall exposes residual kaolinite clays similar to those beneath the beanfield. These exposures were used for *in situ* determinations of resistivities to help constrain the resistivity interpretations in the beanfield. The beanfield and farmyard areas are collectively known as the Munsell property, after the name of the property owner.

Acknowledgements

This study supplemented a kaolin resources assessment program that was conducted by the Natural Resources Research Institute (NRRI). Support for this study was provided by the Natural Resources Research Institute, the Legislative Commission on Minnesota Resources, and the Minnesota Geological Survey. We gratefully acknowledge Mr. William Munsell of Franklin, Minnesota, for access to his property. Field work was conducted during October 10-13, 1988. Split-tube auger drill core was provided by the Northwestern States Portland Cement Company of Mason City, Iowa, and their donation is gratefully acknowledged.

GEOLOGY

Bedrock Geology

Outcrops of rock types that are thought to be representative throughout the Munsell property are plentiful at the north end of the geophysical grid (Plate 1A). The rocks are exposed in an east-west trending ridge that stands about 40-50 feet above the surrounding Minnesota River floodplain. Outcrops were mapped at a scale of 1"=50' and tied into the geophysical grid system using a pace and compass method. Outcrops, inferred contacts, and thin section sample locations are shown on Plate 1. Two major rock types are present in the ridge: 1) quartz monzonite that is Archean in age; and 2) basaltic dikes that are early Proterozoic. Both are easily weathered in the area but as Lund (1950, p.32) observed "... the granular texture of the [quartz monzonite] causes it to disintegrate and makes it more susceptible to erosion than the fine-grained tough basalt".

The monzonitic rocks of the area were mapped by Lund (1950) as Morton Quartz Monzonite Gneiss. He noted a highly contorted structure in the rock and the presence of numerous basic inclusions. However, the rocks mapped in the Munsell property do not exhibit any type of gneissic structure; rather, they are a medium- to coarse-grained, equigranular, quartz monzonite that locally grade into zones of granite and granodiorite. The rock has a generally homogeneous texture throughout the area, but local pegmatitic pods with quartz veins may be present.

The monzonite is easily weathered and commonly breaks along highly irregular subhorizontal planes that are referred to as "hackly fractures". These generally trend N 80EE with dips of 5-20E S, but steeper dips (up to 40E) and

variable strikes (N 50-85EW) are present locally. Minor near-vertical planar joints are also present in the monzonite and can be broken into three groups: 1) N 0-40EW (6 measurements); 2) N 65-70EW (2 measurements); and 3) N 40-60EE (2 measurements).

Minor inclusions of banded biotitic quartz diorite gneiss (gag unit of Lund, 1950) are noted at two localities and range in size from 0.2 X 0.3 to 0.9 X 1.5 meters across (sample M-6 was collected from the latter). At one locality (sample M-4), the monzonite is highly indurated due to the presence (20%) of a cryptocrystalline mixture of quartz and plagioclase in addition to the constituent minerals. This outcrop is also located in close proximity to an inferred NE-trending fault zone but is devoid of any joints or hackly fracture. The relationship of the fault to the highly indurated quartz monzonite is poorly understood at present.

In thin section, the quartz monzonite is characterized by a medium- to coarse-grained mixture of plagioclase, microcline and quartz ± biotite. The constituent crystals exhibit curvilinear, mutually interfering grain boundaries, and the quartz occurs as polycrystalline grains with moderately sutured internal grain boundaries. Table 1 lists the approximate amounts (visual estimate) of minerals present in seven quartz monzonite samples. Note that two of the samples (M-12B, M-12W) come from the southeast corner of the Munsell property and are not from the ridge. Both samples come from room-sized boulders, which are extremely abundant and piled on top of each other in the southeast corner of the property. Although the boulders are not true outcrops, it is believed that they are very close to their immediate source area. Scattered crude gneissic banding is present in the boulders, but the chaotic arrangement of the banding from boulder to boulder suggests that some

rotation of the boulders has occurred. A mechanism of spheroidal weathering, coupled with selective winnowing of the intra-boulder material, is envisioned in explaining the reason for the southeast boulder/outcrop area.

Table 1.

QUARTZ MONZONITES – MODAL PERCENTAGES

SAMPLE NUMBER	PLAG.	K–SPAR	QUARTZ	BIOTITE	MISCELLANEOUS
M–2	20%	53%	25%	2%	
M–4	25%	35%	20%	–	20% cryptocrystalline qtz. and feld.
M–5	51%	20%	25%	4%	
M–6	72%	10%	15%	3%	BDI inclusion
M–10	50%	40%	10%	tr	
M–11	30%	30%	39%	1%	
M–12B	15%	60%	20%	5%	boulder – SE area
M–12W	21%	60%	15%	4%	boulder – SE area

Also included in Table 1 is a sample of an inclusion of banded biotitic quartz diorite gneiss (sample M-6). In thin section, the inclusion exhibits a vastly different texture (than the enclosing quartz monzonite) characterized by medium-grained crystals of plagioclase, quartz, and microcline, all of which occur as subrounded grains that give the rock a sedimentary appearance.

In all samples, the plagioclase has been severely altered to sericite and clays, which give the mineral a cloudy/dusty appearance. Conversely, the microcline is generally "fresh" but in some samples exhibits a similar alteration but to a lesser degree (weak to moderate).

An east-west trending dike of basalt is the dominant feature of the exposures in the ridge. It is a single dike along the eastern half of the ridge that divides into

two separate dikes toward the west (on the immediate east side of the fault) (Plate 1A). The dikes are highly indurated and characterized by a fine- to medium-grained, dark-colored rock containing plagioclase, augite, hornblende, quartz, and minor amounts of chlorite (after augite), magnetite, pyrrhotite, chalcopyrite, pyrite, calcite, and apatite. Table 2 lists the percentages of minerals present (visual estimation) in four thin sections. Plagioclase is the dominant mineral and occurs as slender laths that are often strongly altered to sericite, clays, and calcite. Augite is the second most common mineral and occurs as euhedral to anhedral crystals (often twinned) that interpenetrate with the plagioclase laths. Chlorite ± epidote and serpentine alteration of the augite is common. Minor amounts of hornblende is also present in the thin sections. Quartz is also a major constituent of the dikes and occurs as highly irregular and embayed oikocrysts.

Table 2.

BASALT DIKES – MODAL PERCENTAGES

SAMPLE NUMBER	PLAG.	AUGITE	HNBL	QTZ	CHLORITE	MAG	SULF
M–1	60%	20%	6%	10%	1%	tr	3%
M–3	55%	15%	3%	1%	15%	1%	tr
M–7	60%	20%	5%	5%	10%	2%	tr
M–9	60%	28%	1%	5%	3%	3%	tr

Several joint patterns are present within the dikes and show a wide variety of orientations. Most of the thirty-one joint measurements fall within two categories: N 25EE (12 measurements in the N 10-45EE range) and N 80EW (14 measurements in the N 80EE to N 55EW range). As mentioned above, the dikes are less weathered than the surrounding quartz monzonites because they are finer grained and contain

interpenetrating crystals and quartz oikocrysts. The dikes are also variably magnetic due to accessory amounts of magnetite and pyrrhotite.

Regional Clay Geology

The clay occurrences in the Minnesota River Valley are composed of three classes of materials:

1. Residual/saprolite and secondary kaolinitic clays
2. Cretaceous shales
3. Glacial till and lake sediments

All three types of material are found on the Munsell property and are examined as part of this and a previous LCMR clay study (Heine, *et al*, in prep.).

The residual and secondary kaolinitic clays were formed during a period of weathering and reworking prior to the deposition of the glacial till and sediments (3 above). The residual kaolinitic material is a saprolite developed on a weathered bedrock surface. This material is composed of varying amounts of clay and partially weathered to unweathered minerals from the parent rocks. The saprolite thickness varies from less than 1 to more than 30.5 meters in the Minnesota River Valley and is found well outside this area. The composition of the residuum is dependent on the composition of the parent rock, the degree of weathering, and the depth of erosion. Felsic parent rock weathers to varying amounts of kaolinite, halloysite, illite, quartz, feldspar, and accessory minerals. Mafic protoliths result in mixtures of illite, chlorite, kaolinite, feldspar, and accessory minerals. The degree of weathering and its depth control the proportions of the minerals, and the parent rock controls the overall composition. The residual clays are Parham's (1969) Unit 1.

The secondary kaolinitic shales are part of Parham's Unit 2. This package of rocks is made up of kaolinitic sandstones, kaolinitic shales, pisolitic kaolinitic shales, and iron-stained pisolitic shales. The secondary clay thickness varies from less than 1 to 13.7 meters in the Minnesota River Valley. The clay mineralogy is commonly kaolinite, halloysite, quartz and feldspar, with gibbsite and boehmite in the pisolitic rocks, and hematite in the iron-stained rocks. Illite and chlorite are rare. These rocks were formed by the reworking of the residual Unit 1 in a fluvial environment.

Late Cretaceous package of rocks include shales, siltstones, sandstones, lignites, and a discontinuous bentonite. These rocks range in thickness from less than 1 to more than 5.5 meters in the Minnesota River Valley. The shales vary from silty to clay-rich and have a moderate to high organic content, which gives them a distinctive grey to black color. The dominate clay mineral is kaolinite, with trace to minor amounts of illite, chlorite and mixed-layered clays. In general, the amount of kaolinite decreases upward in the Cretaceous sediments. The Cretaceous sediments were deposited in various environments, from terrestrial to paludal and marine, related to the drowning of the area by the Western Cretaceous Seaway. These rocks are Unit 3 of Parham's (1969) study of the kaolin clays in Minnesota.

The glacial materials are chiefly clay-sized rock flour and pulverized rock, with the amount of clay varying with the style of deposition. The glacial sediments are calcareous and easily distinguishable from older materials. Glacial till contains less clay-sized material than does glacial lake material. Glacial materials in the Minnesota River Valley are related to the Altamont moraine association of the Des

Moines Lobe. These materials have a thickness of less than 1 to more than 24 meters in this area.

Munsell Property Clay Geology

Quartz monzonite with gneissic inclusions crops out in the beanfield (Plate 1A), and drill core was donated by the Northwestern States Portland Cement Company of Mason City, Iowa (Appendix A). The farmyard (Plate 1B) is located to the southeast of the beanfield and contains outcrops of residual quartz monzonite, granitic gneiss, and mafic dikes; a road cut to the west exposes residual and secondary kaolinitic clays.

Munsell Beanfield

Drill holes in the Munsell beanfield show that there is at least 0 - 13 meters of residual clay (Fig. 1). This material is variable in composition, having both felsic and mafic parent rocks. The relationship of felsic and mafic rocks is similar to that observed in the bedrock outcrops north of the field.

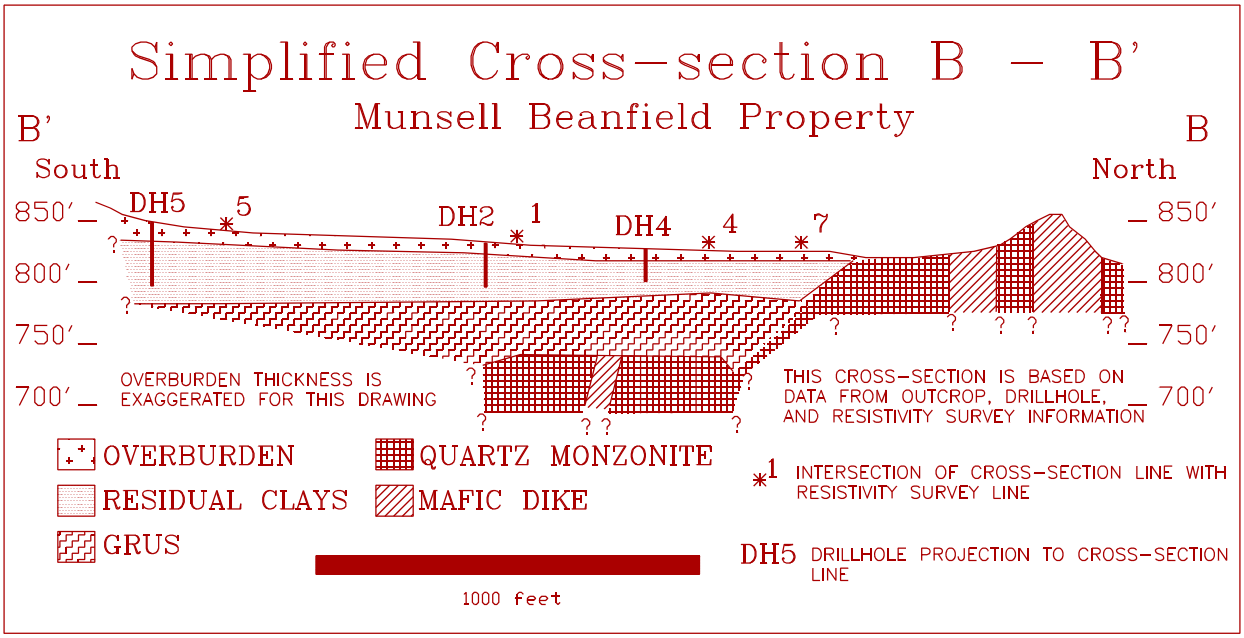

Figure 1. Geologic cross-section of the Munsell beanfield property, Franklin, Redwood County, MN.

The residual clay is composed of kaolinite, quartz, biotite, and feldspar. Also present was a greenish-yellow clay-rich material, which is thought to be a mixture of kaolin, illite, and a mixed-layered clay. X-ray analysis of the 2-micron fraction of similar material from the Munsell farmyard outcrops (Plate 1B) identified kaolin as the major clay mineral, with minor to trace amounts of illite, and a mixed-layered clay (Heine, *et al*, in prep.). The greenish-yellow clay was not X-rayed separately. Examined visually, the clay content ranges from 50% to 90% and decreases with depth. In whole pieces of core, some of the residual clay displays relict gneissic banding and appears very similar to residual clays associated with typical Morton Gneiss. Other core fragments exhibited a granitic texture similar to the quartz monzonite.

The weathered mineralogy of the mafic dikes that crop out north of the beanfield is also recognized in the drill cores. This material is composed of a dark

green clay, feldspar, biotite, and minor kaolinite. A similar weathered dike occurs about 1.2 kilometers southeast in the Northern Con-Agg kaolin mine, but its clay mineralogy is mostly kaolinite, with minor to trace amounts of illite, chlorite, and a mixed-layered clay. The orientation of the dikes in the drill holes is not known. However, in outcrop, the dikes strike about east-west.

There is a very thin (6 cm) zone of reworked kaolinite in drill hole #7. This clay is post-glacial in origin and is not related to the secondary kaolinites of Parham's (1969) Unit 2. Visual composition is 74% kaolinite, 20% feldspar, and 6% quartz. The quartz and feldspar grains are subangular and form a crude bedding that is matrix supported by kaolinite. This reworked kaolinite does not occur in the other drill holes. This material is a local reworking by runoff of the residual kaolinitic clay in the beanfield that is overlain by a clay-rich gravel.

Munsell Farmyard

The Munsell farmyard (Plate 1B) contains outcrops of quartz monzonite, granite gneiss, biotite schist and mafic dikes, all of which have undergone some weathering. The least weathered outcrop is in the eastern part of the farmyard. West of the farmyard proper, a drill road is cut into the hillside. Along this cut, residual kaolinitic clays, similar to clays observed in the beanfield drill holes, crop out. A thin layer of secondary kaolinite occurs between the saprolite and the overlying basal till. Farther west along the road is a zone in the basal till that contains disturbed Cretaceous shale. On the farmyard property, the rocks become more intensely weathered from east to west (Fig. 2).

In the farmyard all the outcrops exhibit some degree of weathering. The eastern third has the least weathered rock--a quartz monzonite, with gneissic inclusions similar to outcrops north of the beanfield. The mafic dike that cuts this outcrop is also similar to the beanfield mafic dikes. Both rock types are weathered, showing some bleaching. The quartz monzonite, gneiss and dike are friable and disintegrate along grain boundaries. At the east end of the outcrop area, the feldspars are pink and weather to clay. West along this outcrop, the rock is progressively weathered to grus and residual clay over a distance of 137.2 m (450 ft.; Fig. 2).

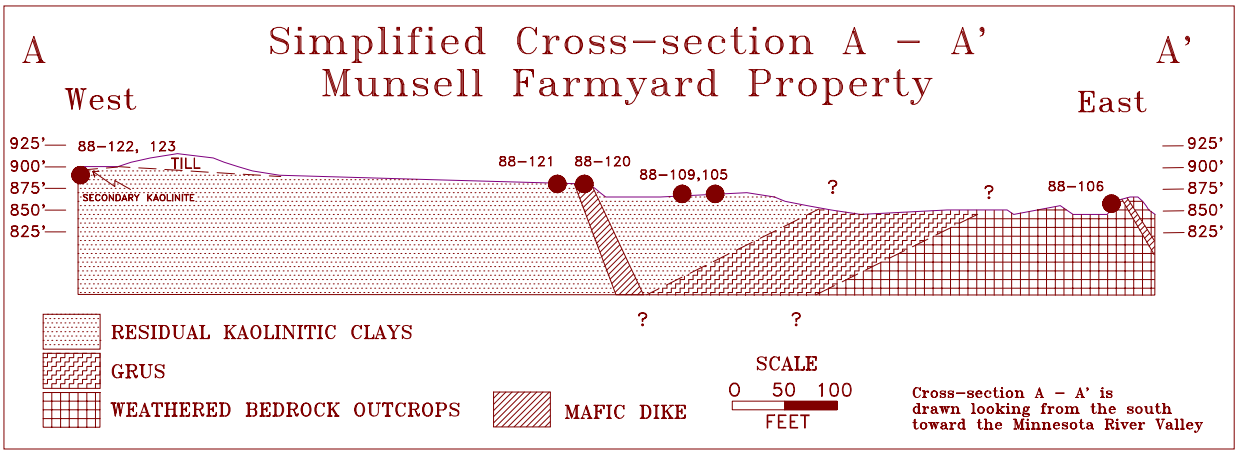

Figure 2. Geologic cross-section of the Munsell farmyard property, Franklin, Redwood County, MN.

This weathering progression starts as a formation of clay along grain boundaries and on cleavage surfaces of feldspar. With further weathering, quartz and feldspar and minor biotite are the coarse material in a matrix of kaolinitic clay. The coarser feldspar is highly weathered in this material and generally consists of 1- to 3-mm fragments. Feldspar crystals larger than 8 cm are still found in parts of the weathered gneiss and residual clays; they appear more resistant to weathering than the smaller feldspars in the quartz monzonite. This is probably the result of

compositional difference between the feldspars. Relict textures of granitic and gneissic origin are displayed in all of the outcrops. South of the main farmyard outcrop is a small outcrop containing both gneiss and biotite schist. Both are weathered to grus and still contain strong, foliated, original textures.

To the west of the farmyard, a drill road cuts through residual clays that have both relict granitic and gneissic textures. Just north of the drill road is a trench along the contact of a mafic dike and residual kaolinitic clay. The dike material, on the east side of the trench, can be disintegrated with some difficulty. On the west side of the trench, the bank is composed of residual kaolinitic clay similar to the western outcrop in the farmyard area. In this area, the felsic rock is more highly weathered than the mafic dike. Along the drill road, there are additional exposures of residual clay. Approximately 146.3 meters southwest of the mafic dike, the drill road cuts through 1.1 meters of secondary kaolinite that overlies a residual kaolinitic clay with granitic textures. This secondary clay contains 57% clay (Heine, *et al*, in prep.). Kaolinite is the only mineral identified by X-ray analysis of the <2-micron fraction. This secondary clay is overlain by glacial till which exposed along the rest of the road to the west. The till is overlain by glacial outwash.

The Munsell farmyard has an interesting cross section from east to west (Fig. 2). The outcrops in the east are slightly weathered. The rocks are progressively more weathered toward the west. Finally, reworking formed a secondary kaolinitic clay before the entire section is truncated by the glacial material. The difference in elevation from the east end to the west is only 30 feet or 9.1 meters (855 ft./260.6 m in the east, 885 ft./269.7 m in the west) over a distance of 335.3 meters. This section is similar to a vertical profile from bedrock through saprolite and into a

secondary kaolinitic shale, providing a good example of the gradual changes that occur due to weathering.

ELECTRICAL RESISTIVITY SURVEYING

Electrical resistivity is measured by placing a current into the ground through two electrodes and observing the drop in potential through two other electrodes. The apparent resistivity of the subsurface is a function of resistivity variations at depth and as such can be used to investigate subsurface structure. Kaolin is an electrically conductive clay that contrasts markedly with the bedrock protolith, and thus should be highly amenable to electrical resistivity surveying. Electrical resistivity sounding was used to estimate the thickness of the kaolin, and profiling was used to detect lateral variations. Kaolin as used in this study indicates the kaolinite-rich residuum or saprolite.

In electrical resistivity sounding, successive readings are taken while changing the electrode spacing relative to a stationary center. As the array is expanded, more of the current goes deeper. Therefore, by inspecting the total sounding curve, interpretations can be made about vertical variations in resistivity. In this study a Wenner electrode array was used, which consists of current electrodes spaced at 3a/2 and potential electrodes spaced a/2, relative to the center of the array. Resistivity soundings were conducted at seven sites over the beanfield (Plate 1A). The a-spacing on the array was expanded from 0.914 meter (3 ft.) to 91.44 meters (300 ft.) and, in order to check for lateral inhomogeneities, Lee configuration readings (left and right) were included at every a-spacing (Appendix B). A further check for lateral inhomogeneities at some sites consisted of partial to full Wenner soundings that were perpendicular to the original spread. The resistivity

data were converted to metric units (Appendix C) and plotted on a log-log scale (Figs. 3-9).

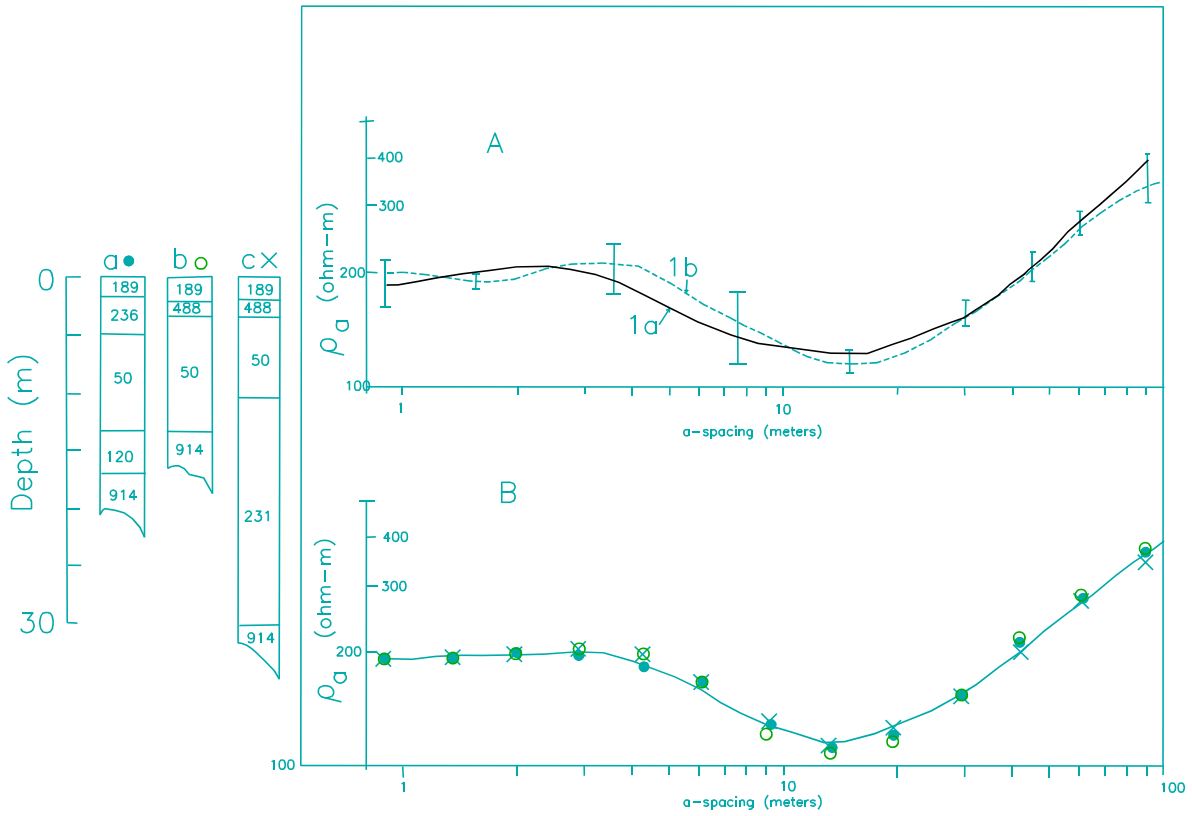

Figure 3. Wenner sounding 1. (A) Vertical lines represent reading positions and their length represents the range of Lee right and Lee left values. Line 1a is the east–west traverse; line 1b is the north–south traverse. (B) Average of the orthogonal soundings in (A) (curve) and values associated with models (symbols along curve). Models are shown at left.

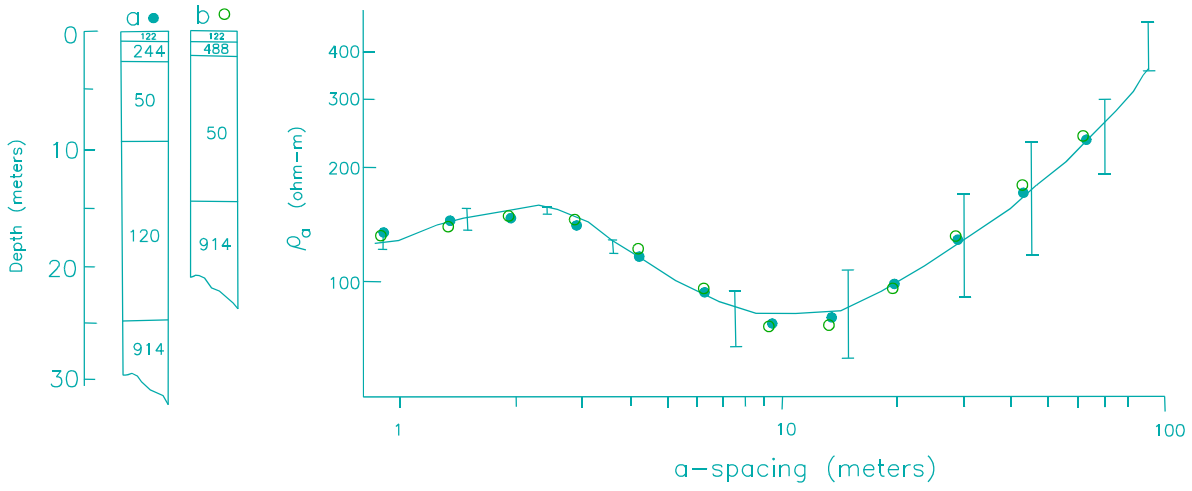

Figure 4. Wenner sounding 2. Vertical lines represent reading positions and their length represents the range of Lee left and Lee right values. Models are shown at left and model values shown as symbols along the curve.

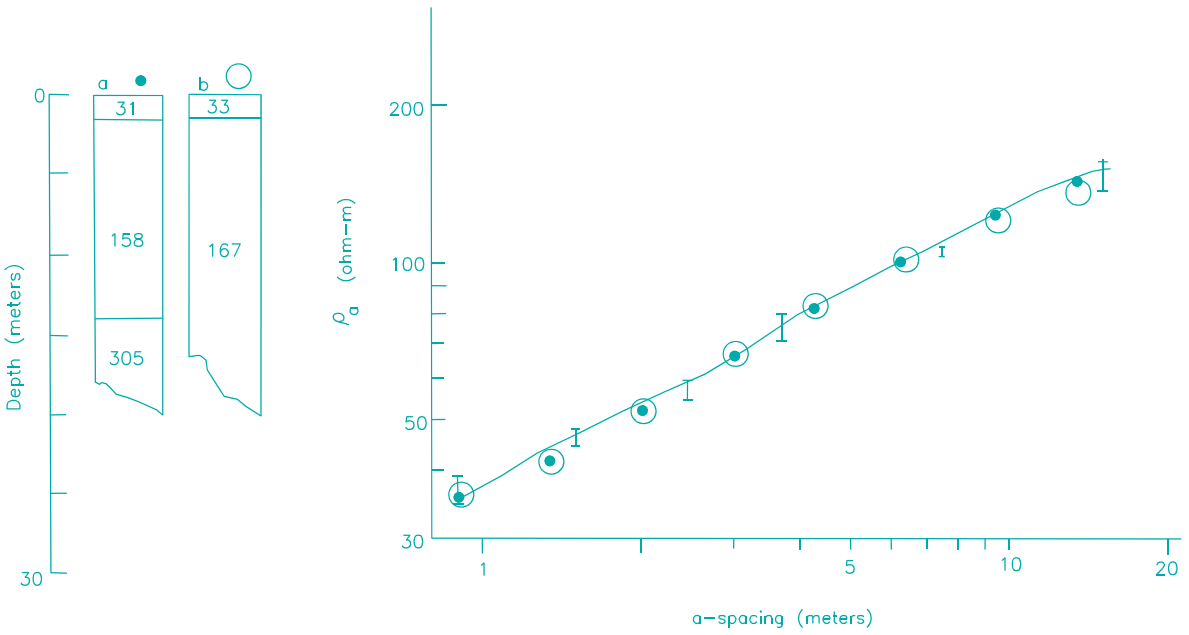

Figure 5. Wenner sounding 3. Vertical lines represent reading positions and their length represents the range of Lee left and Lee right values. Models are shown at left and model values shown as symbols along the curve.

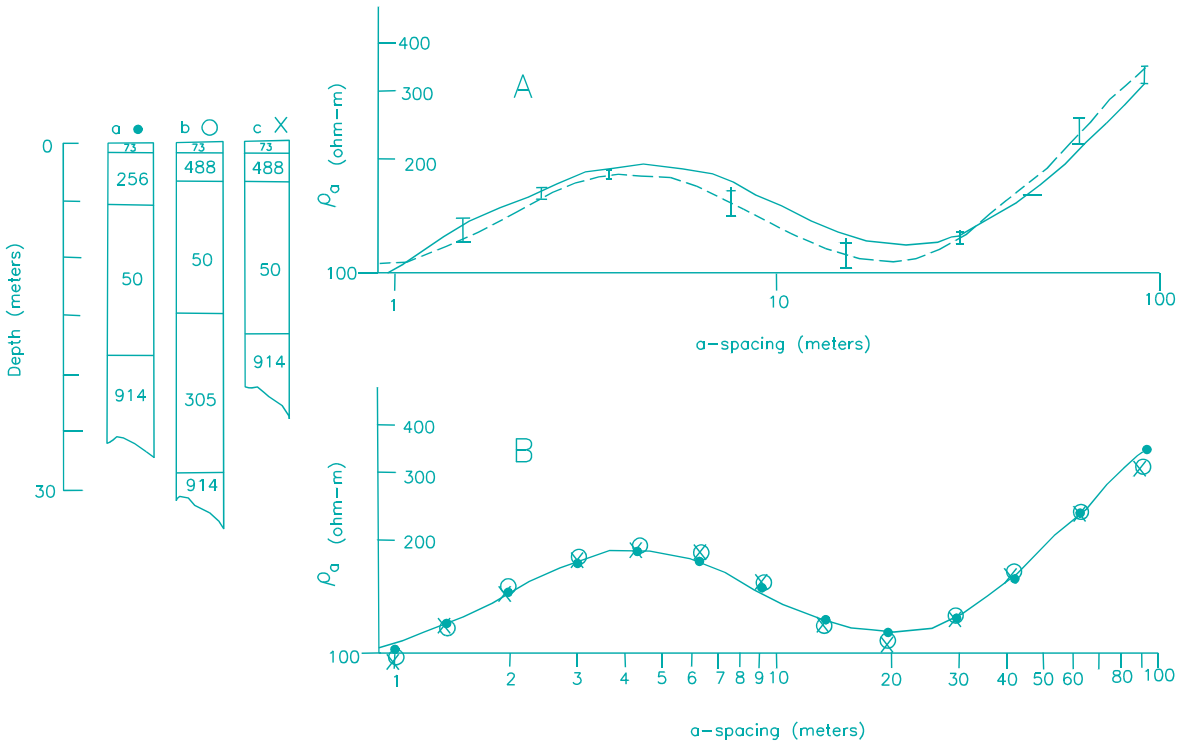

Figure 6. Wenner sounding 4. (A) Vertical lines represent reading positions and their length represents the range of Lee right and Lee left values. Line 4a is the east-west traverse; line 4b is the north-south traverse. (B) Average of the orthogonal soundings in (A) (curve) and values associated with models (symbols along curve). Models are shown at left.

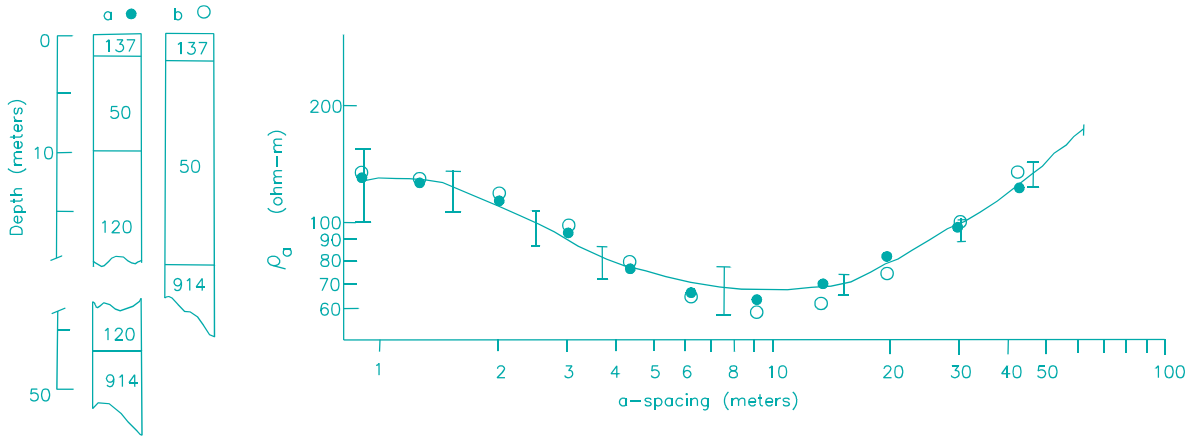

Figure 7. Wenner sounding 5. Vertical lines represent reading positions and their length represents the range of Lee left and Lee right values. Models are shown at left and model values shown as symbols along the curve.

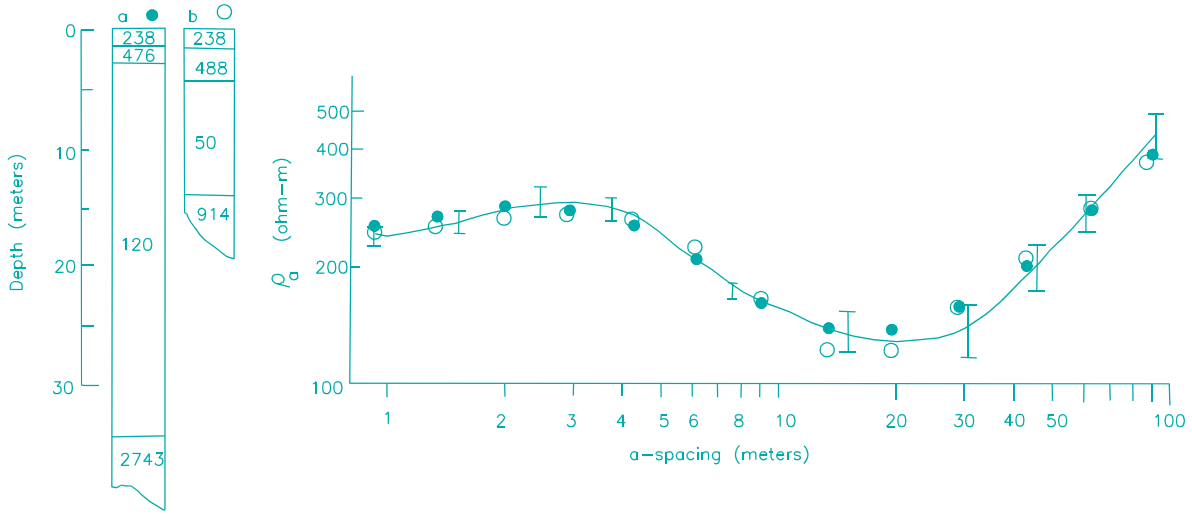

Figure 8. Wenner sounding 6. Vertical lines represent reading positions and their length represents the range of Lee left and Lee right values. Models are shown at left and model values shown as symbols along the curve.

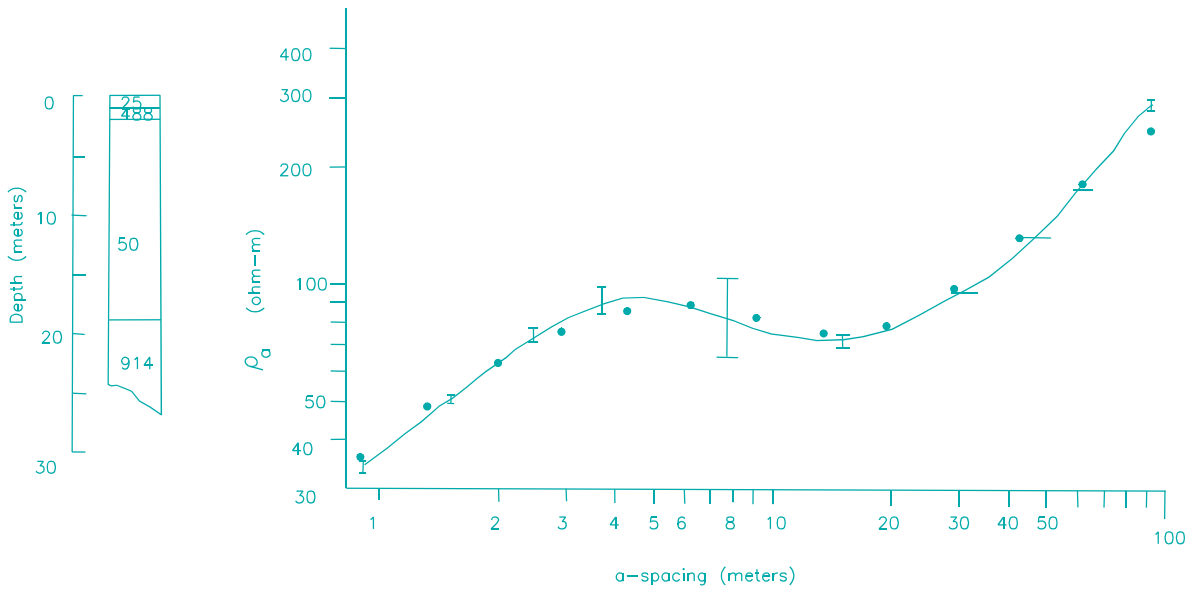

Figure 9. Wenner sounding 7. Vertical Lines represent reading positions and their length represents the range of Lee left and Lee right values. Models are shown at left and model values shown as symbols along the curve.

The interpretations of these curves were constrained by a series of direct resistivity determinations that were made using short Wenner spreads (a=0.91-15.24 m) at exposures of representative units in the farmyard (Plate 1B; Figs. 11 and 12). All interpretations assumed horizontal layering and followed a preliminary analysis using master curves (Orellana and Mooney, 1972). The soundings were interpreted using a resistivity inversion program based on Marquardt's algorithm (Davis, 1979). The models were then evaluated by comparing them to the drill hole data (Plate 1A; Table 3).

Electrical resistivity profiling involves moving the array along a grid but keeping a constant electrode spacing. In this study the Wenner array, with an a-spacing of 30.48 meters, was moved along lines 0, 4E, and 8E in the beanfield. The selected a-spacing was based on some general rules of thumb (Mooney, 1980) and expected thicknesses as known from drill hole data (Table 3). Full-spread readings were taken every 30.48 meters and the apparent resistivity was plotted at the center of the spread. The readings are included in the field notes (Appendix B), and the results are plotted in Figure 12.

Table 3. Summary of Drill Hole Data

Drill Hole #	Overburden Thickness (m)	Kaolin Thickness (m)	Protolith	Material at Bottom
1	1.37	11.13	gneiss	kaolin
2	2.59	7.62	gneiss	grus
3	1.55	12.92	gneiss; some mafic dike	kaolin
4	2.44	5.64	mafic dike; minor gneiss	grus

5	5.18	11.43	gneiss	grus
7	1.31	9.20	gneiss	grus
8	2.29	5.79	gneiss	grus
9* (no log)	1.5 approx.	0.00	------	grus

*Note: Drill hole 9 is near resistivity spread 3 on Plate 1A.

Interpretation of Short Soundings in the Farmyard

The red grus has clay only along fractures, and its divergent apparent resistivity ranging from 230 to 860 ohm meters (Fig. 10) reflects its heterogeneous nature. Nonetheless, the asymptotic resistivity maximum, which is interpreted to be 914 ohm meters, is reasonable for a fresh to slightly weathered crystalline rock. The kaolinitic grus has a prominent plateau on the sounding curve that implies a resistivity of about 120 ohm meters. Soundings 10 and 11 are in the kaolin, and plateaus on both curves indicates local resistivity of around 50 ohm meters. The small pod of Cretaceous clay atop the kaolin at sounding 12 (Fig. 10) has an extremely low resistivity of 25-30 ohm meters, but this clay does not appear to be a major component of the deposit beneath the beanfield. Glacial till (Fig. 11), sampled by spreads 13 and 14, is absent in the beanfield, but the results have important implications for any exploration outside the Minnesota River Valley where till typically overlies the kaolin. Some material in the till is even lower in resistivity than the kaolin and would therefore mask the kaolin signature.

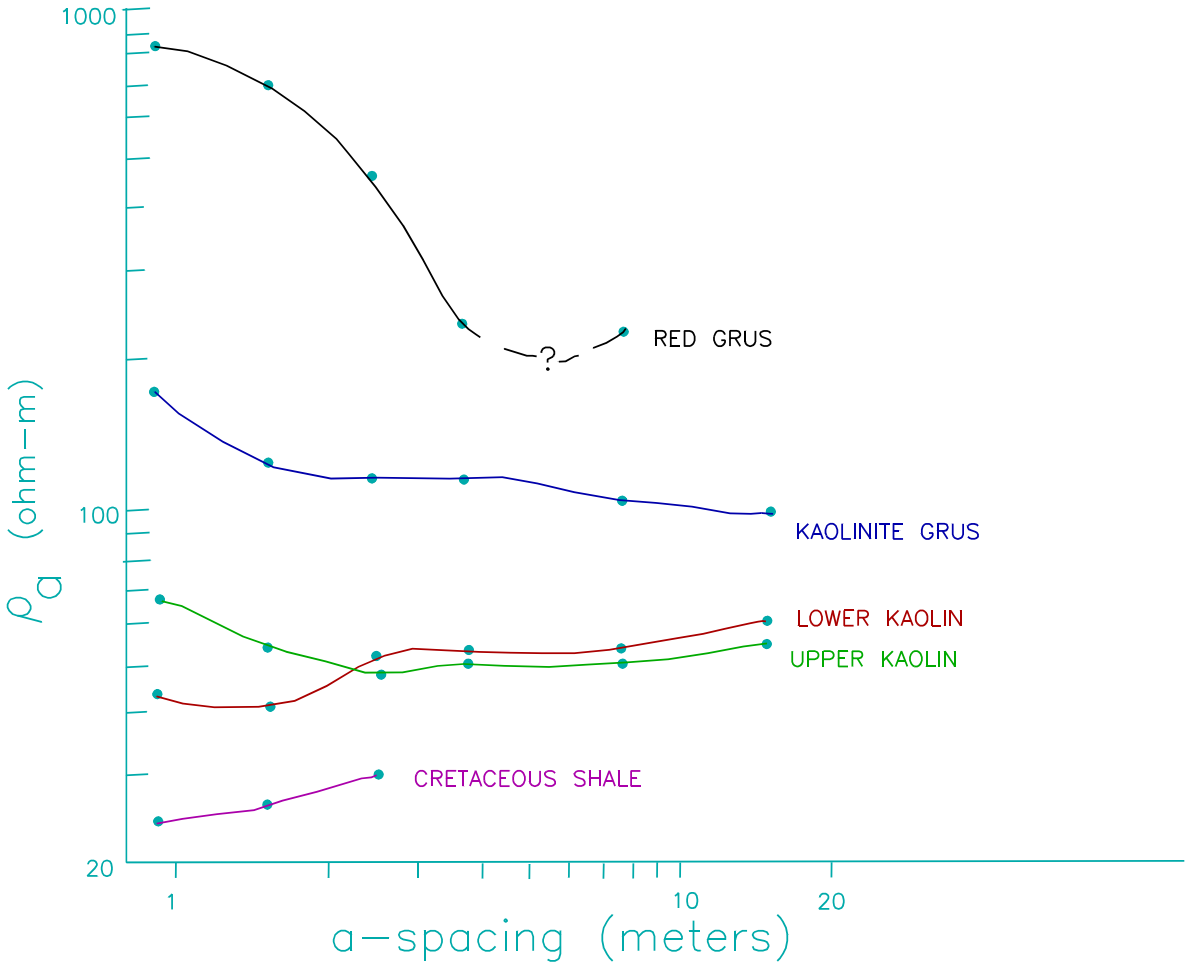

Figure 10. Short Wenner soundings taken from representative units exposed near the northwest corner of Section 30, T. 112 N., R. 33 W. Dots represent actual readings.

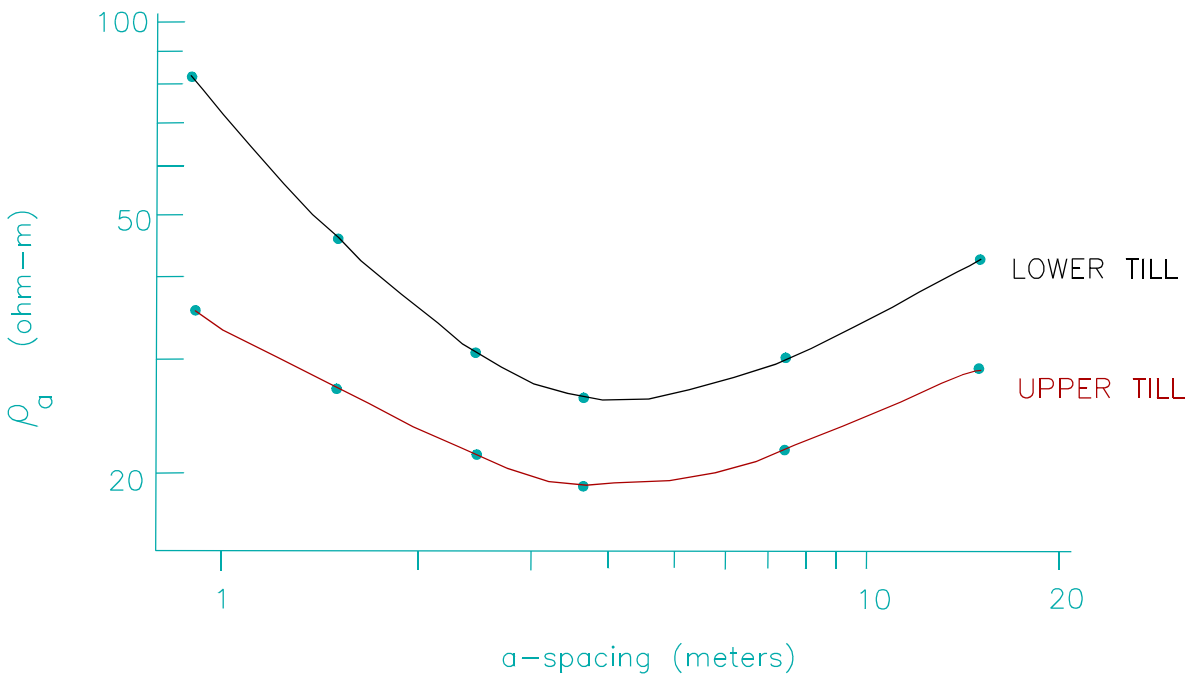

Figure 11. Short Wenner soundings taken from exposures of glacial till near the northwest corner of Section 30, T. 112 N., R. 33 W. Dots represent actual readings.

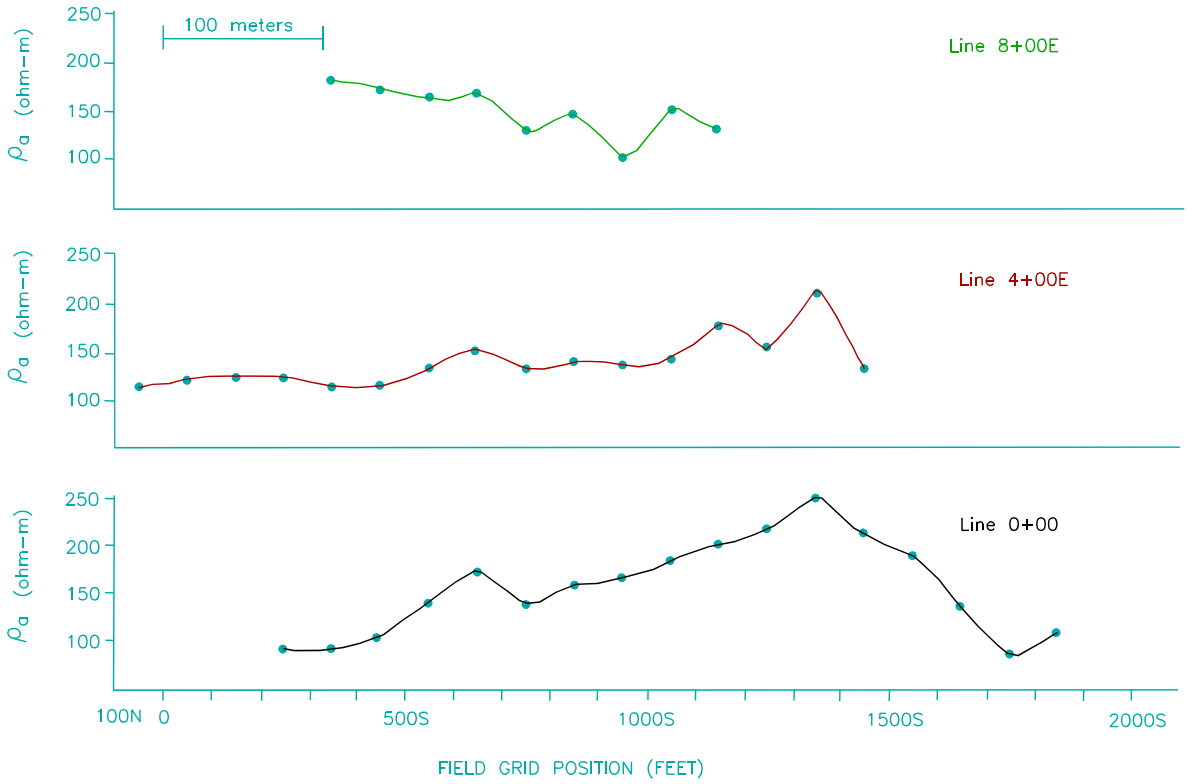

Figure 12. Results of moving the Wenner array along lines 0+00, 4+00E, and 8+00E using an a-spacing of 30.48 meters.

Interpretation of Soundings Inside the Beanfield Area

Except for curve 3, the sounding curves within the beanfield are grossly similar in form, consisting of a plateau or a rise to a minor high at shorter a-spacings, and a broad low followed by a sharp climb at longer a-spacings (Figs. 3-9). Considering the general stratigraphy from the drill hole data (Table 3), the plateau or minor high most likely reflects overburden, the broad low reflects the kaolin, and the sharp climb reflects the transition into fresh bedrock. Scatter in the Lee determinations at short a-spacings for soundings 1, 4, 5, 7 and at long a-spacings for soundings 2 and 6 indicates local departures from a horizontally layered sequence (Figs. 3-9), and the interpretations should be regarded with appropriate caution. Models were fitted to all sounding curves and ambiguity was investigated by creating more than one model for most curves. The resistivities of the red grus, kaolinitic grus, and the kaolin that were measured directly on exposures (Fig. 10) were incorporated into the models, and the models were adjusted to fit the curve.

No samples or resistivity data were available for the overburden in the beanfield, and so the resistivity of the shallowest overburden was simply estimated from the apparent resistivity observed at the shortest a-spacing. The minor highs at short a-spacings (Figs. 3, 4, 6, 8, and 9) imply a resistive layer overlying the kaolin, and its resistivity was estimated by fitting two-layer curves of Orellana and Mooney (1972); the two-layer overburden derived this way is shown in the models. However, overburden thickness derived this way appeared to be over estimated; *model a* for sounding 1 yields an overburden thickness of 5.07 meters (Fig. 3), whereas drill hole 2 near the center of the sounding intersected only 2.59 meters of

overburden. Increasing the resistivity of the deeper overburden from 236 to 488 ohm meters decreased the total overburden thickness to 3.47 meters, or to within a meter of the depth in the drill hole, and this resistivity was favored in subsequent models. The high resistivity interpreted for the deeper overburden is consistent with sandy material, perhaps outwash or alluvium.

There can be significant ambiguity in determining the thickness of kaolin from resistivity data, with the greatest problem lying in the transition from kaolin to fresh rock. The placement of conductive kaolin (50 ohm meters) directly on fresh and resistive rock (914 ohm meters) tends to thicken the modeled kaolin layer, whereas the insertion of partially weathered layers with intermediate resistivities (120-305 ohm meters) tends to thin the kaolin (see models on Figs. 3-9). An extreme case occurs for sounding 6 where an abrupt transition to fresh basement yields a kaolin thickness of 9.86 meters (*model b*, Fig. 8), whereas the insertion of an intermediate resistivity layer (120 ohm meters) causes the kaolinitic layer to be totally squeezed out by the inversion program (*model a*, Fig. 8). Support for a thick transition zone occurs at sounding 3 (Fig. 5), where shallow bedrock (see drill hole 9 in Table 3) is interpreted to have a somewhat low resistivity of 158-167 ohm meters down to the depth of at least a few meters. On the other hand, an intermediate resistivity layer at the base of the kaolin was squeezed out by the inversion program for sounding 7 (Fig. 9), and thus the transition to fresh bedrock may be sharp in places. Running several different models for each sounding makes it possible to estimate a range of likely thicknesses.

The interpretations of the soundings (Figs. 3-9, and Table 4) agree reasonably well with drill hole data (Table 3). At the north end of the field, where

soundings 4 and 7 indicate kaolin thicknesses of 11.57-13.37 meters and 17.08 meters, respectively, drill hole 3 penetrated 12.92 meters of kaolin before drilling ceased. At the south end of the field, where sounding 5 indicates a kaolin thickness of 7.85-17.50 meters, drill hole 1 penetrated 11.27 meters of kaolin before drilling stopped. Generally thinner kaolin is indicated in the central part of the field, where soundings 1, 2, and 6 indicate thicknesses of 6.97-10.23, 7.10-12.89, and 0-9.86 meters, respectively, drill holes 2, 4, 7, and 8 penetrated kaolin thicknesses of 7.62, 5.64, 9.20 and 5.79 meters, respectively, prior to bottoming out in grus.

Table 4. Summary of Resistivity Models

[E, layer thickness in meters; P, resistivity in ohm meters; numeric subscripts in order of increasing depth]

Model	E_1/P_1	E_2/P_2	E_3/P_3	E_4/P_4	E_5/P_5
1a	1.76/189	3.26/236	8.33/50	3.82/120	inf./914
1b	2.13/189	1.34/488	10.23/50	inf./914	---
1c	2.13/189	1.34/488	6.97/50	20.18/231	inf./914
2a	0.93/122	1.40/244	7.10/50	15.67/120	inf./914
2b	1.20/122	0.65/488	12.89/50	inf./914	---
3a	1.24/31	12.80/158	inf./305	---	---
3b	1.32/33	62/167	inf./914	---	---
4a	0.70/73	4.91/256	13.07/50	inf./914	---
4b	0.93/73	2.30/488	11.57/50	13.67/305	inf./914
4c	0.93/73	2.33/488	13.37/50	inf./914	---
5a	1.94/137	7.85/50	36.96/120	inf./914	---
5b	2.08/137	17.50/50	inf./914	---	---

6a	1.13/238	1.58/476	31.70/120	inf./2743	---
6b	1.60/238	2.48/488	9.86/50	inf./914	---
7	0.82/25	0.87/488	17.05/50	inf./914	---

Interpretation of Profiling Data

Although the three profiles (Fig. 12) are not adequate for generating a map, they provide a qualitative perspective on kaolin thickness in the study area. The profile along line 00 has prominent lows at its north and south ends that are consistent with the thicker kaolin indicated by the drill hole and sounding data. Similarly, a broad irregular high over the central part of line 00 is consistent with a thinning of the kaolin and a rise in elevation of fresh bedrock, with the thinnest kaolin around position 1350 S. Profiling along line 4E yields a low at the north end and an irregularly high pattern over the central part. In contrast, line 8E is high at the north end, consistent with the lack of kaolin and shallow bedrock indicated by sounding 3 and drill hole 9. The south end of the 8E line, which is generally low but irregular, possibly indicates an irregular thickness for the kaolin.

GRAVITY SURVEYING

Because of its low density relative to fresh bedrock, kaolin can be investigated by the gravity method. In the Minnesota River Valley, Fogelson (1956) found average densities of 1.99 gm/cc for kaolin and 2.71-2.85 gm/cc for fresh granitic and gneissic rock. If we assume a density contrast of 0.70 gm/cc from a Bouguer slab approximation, a 10-meter change in kaolin thickness should produce an easily detectable anomaly of 0.29 milligal. Besides delineating the geometry of the kaolin deposit, the gravity method may be useful in detecting mafic rocks, which typically weather to poor-quality kaolin in the saprolite.

The gravity data were acquired using a LaCoste-Romberg G-320 meter. Prior to the survey the sensitivity and levels on the instrument were checked and adjusted, and during surveying care was taken during leveling and reading to ensure high precision. Gravity stations were taken at intervals ranging from 30.48 meters up to 91.44 meters along lines 2 West, 00, 2 East, and 4 East (Plate 2), and base checks were conducted at intervals of 1.0 to 1.5 hours. The data were tied into the state gravity network by a single loop to a previously used field base established by Beltrame and others (1982) at the center of the eastern margin of Section 16, T. 112 N., R. 34 W. The gravity data were reduced using the 1971 International Gravity Formula, and two versions of the Bouguer anomaly data produced, one using standard density of 2.67 and a sea level datum (Appendix C), and the other using a local density of 2.00 and a datum of 250.48 meters (821.8 ft.; Plate 2). The latter yielded a Bouguer correction that was more appropriate for the low-density surface material over the kaolin deposits. The precision of the Bouguer

gravity data is believed to be about 0.05 milligal or less. A terrain correction check using Hammer zones B-D indicated that terrain effects were restricted to the ridge at the north end of the prospect, and therefore, no terrain corrections were applied. A regional gravity gradient, estimated to be 0.25 milligal/km from a regional scale Bouguer anomaly map (Ervin, *et al*, 1980), was not removed from the data. Gridding used to make Plate 2 was accomplished using a minimum curvature program provided by the U.S. Geological Survey.

Interpretation of Gravity Data

The Bouguer gravity anomaly data (Plate 2) show a direct relationship to the thickness of kaolin. Between 200 N and 200 S, a sharp gravity gradient occurs just south of an outcrop and most likely reflects a southward thickening of low-density kaolin. This gradient may be enhanced by the effect of the high-density dikes that intrude the gneissic rocks to the north. The closed gravity low south of the sharp gradient corresponds to some of the thickest kaolin in the area, according to drill hole 3 and resistivity soundings 4 and 7 (Plate 1A). This trough of thickened kaolin, as defined by the gravity low, roughly parallels the basalt dikes to the north and could have developed along a dike-related fracture system. A broad plateau in the gravity signature for the central part of the area is consistent with the thin kaolin indicated by drill holes 2, 4, and 8 (Table 3) and by resistivity soundings 1 and 6 (Table 4). This broadly positive signature may be enhanced by "mafic dike" material similar to that encountered in drill hole 4 (Table 3). The southward-decreasing gravity gradient in the southwestern corner of the field (Plate 2) is consistent with the thickened kaolin indicated by drill hole 1 (Table 3) and sounding 5 (Table 4).

MAGNETIC SURVEYING

Although kaolin itself is not magnetic, structures in the Precambrian bedrock that may affect the kaolin could have magnetic signatures. For example, magnetic surveying might be used to detect fracture zones where, because of preferential weathering, kaolin might be thick. The magnetic method may also be useful in detecting mafic dikes or mafic enclaves in the underlying protolith that would have weathered to poor-quality (low kaolinite content) kaolin.

Magnetic readings were taken along the five north-south control lines and along one east-west tie line at 500 S (Plate 3; Appendix D) using a Geometrics model G-826 proton precession magnetometer with the sensor mounted on a 2.44-meter staff. Readings along lines were taken at intervals of 6.095 meters (20 feet) or 15.24 meters (50 feet), depending on observed gradients. Three readings were taken at each station, and temporal variations in the geomagnetic field were monitored at the base stations every 30 to 60 minutes. Each base check consisted of multiple readings taken at intervals of 2-10 minutes. Two base stations tied by looping existed in the survey area, one near stake 200 N along line 00 (which also served as the gravity base) and one at stake 500 S along line 00. All checks indicated subdued geomagnetic field activity. Drift corrections were made by linear interpolation between base checks, tying all survey loops to a datum defined by the first base reading taken during the survey. After these corrections, the intersections of the five north-south lines with the east-west tie line (at 500 S) agreed to within 3 nT, and the data were subsequently contoured at a 20-nT interval (Plate 3). The southern part of the study area was also contoured at an interval of 5 nT (Plate 3)

to show more detail. Gridding for the contouring was accomplished using a minimum curvature program provided by the U.S. Geological Survey.

Magnetic susceptibility data were acquired at exposures at the north end of the study area using an E.D.A. Instruments model K2 magnetic susceptibility meter. These data are summarized in Table 5.

Table 5. Magnetic Susceptibility of Rocks In and Near the Area Studied

Rock Type	Avg. Mag. Susc. ($\times 10^{-3}$ cgs)	Number of Determinations
Magnetic basalt dike	1.26	73
Weakly magnetic basalt dike	0.32	40
Pegmatitic quartz monzonite	0.00	30
Quartz monzonite	0.01	40

Interpretation of the Magnetic Data

The most prominent magnetic signatures are associated with the basalt dikes at the north end of the study area (Plates 1 and 3). Magnetic susceptibility data indicate that the quartz monzonite is essentially nonmagnetic, whereas the dikes are weakly to strongly magnetic (Table 5). Much of the busy signature, consisting of intense and localized highs and lows, doubtless reflects lightning strikes or local concentrations of magnetite, but the consistently negative expression of -100 to -200 nT amplitude over most of the basaltic rock, in spite of a relatively high susceptibility (Table 5), implies a reversed natural remanent magnetization (NRM). South of the dikes a busy but somewhat more subdued signature is evident along

profiles 2W, 00, 2E, and 4W between 0 and 300 S (Plate 3), and it is likely that this signature reflects alluvium from a small stream that originates on the ridge to the north. The tight 300 nT high at 400 S on line 2W (Plate 3) is near a rock and brush pile and may reflect a buried cultural source, but a field check of the area did not locate any such material.

The detailed magnetic map of the beanfield area (Plate 3) shows a magnetic low correlating partly with the gravity low near 400 S on lines 00 and 2E which, as discussed above, is a zone of thickened kaolin that may have developed over a fracture system. However, the extension of the magnetic low to the south does not correlate with any gravity feature. Linear, east-striking magnetic lows along 800 S and 1400 S on the east side of the field and along 1600 S on the west may reflect magnetically reversed dikes that are related to those exposed at the north. The magnetic low along 800 S correlates in part with a gravity high (Plate 2) where drill hole 4 encountered a significant amount of "mafic dike" material (Table 3).

CONCLUSIONS AND RECOMMENDATIONS

Electrical resistivity was useful in exploring a kaolin occurrence. Resistivities were measured directly on nearby exposures in the farmyard of grus, kaolinitic saprolite, Cretaceous clay, and glacial till, and were used to interpret the Wenner soundings. Interpretations were in general agreement with drill hole data. The greatest ambiguity is associated with the downward transition from kaolin (saprolite) to fresh crystalline rock, which may range from gradational over several meters to abrupt. The best solution is to model a sounding both ways, so that a likely range of kaolin thickness can be estimated. Electrical resistivity profiling is sensitive to lateral variations in thickness of the kaolin. Both the sounding and profiling data indicate that the kaolin is thickest at the south end of the prospect and near the bedrock ridge at the north, and is much thinner in the central two-thirds of this area. This finding was supported by results of the drilling.

Gravity and magnetic methods also yield potentially useful information on the kaolin. The gravity data are inversely related to kaolin thickness; prominent lows of 0.15 to 0.25 milligals occur over the thickest deposits near the north and south ends of the field. A broad, positive saddle in the gravity data across the center of the area corresponds to thinner kaolin and may in part reflect mafic dikes cutting the monzonitic and gneissic protolith. Linear magnetic lows across this part of the area may trace mafic dikes related to dikes of reversed polarity exposed to the north. If present, these dikes could locally be associated with poor-quality kaolin.

Of the three methods tested, electrical resistivity appears to be the most sensitive to kaolin thickness, has the least expensive instrumentation (a few

thousands of dollars), and its field acquisition is easiest. An instrument operator assisted by four untrained assistants can rapidly acquire both sounding and profiling data and determine locations simply by pace and compass. In contrast, the gravity method has instrumentation costs nearly an order of magnitude higher, and it requires that elevations be precisely located by surveying. Furthermore, the effect of terrain and regional gravity gradients, although not a problem in this study, could complicate gravity interpretation elsewhere in the Minnesota River Valley.

It must be cautioned that the results of this study cannot be applied to kaolin deposits overlain by glacial till. Some glacial clays are at least as conductive as the kaolin and would mask the electrical signature of the underlying kaolinitic clays. Furthermore, the effect of buried bedrock topography and the lack of geologic control due to the overburden could severely complicate gravity interpretation.

In addition to the methods tested here, several other geophysical methods warrant investigation. Electromagnetic (EM) methods might be used to study thickness variations of the conductive kaolin, and EM data are usually quicker and cheaper to acquire than resistivity data. Because clays have a membrane polarization, induced polarization should be useful in studying the thickness and quality of kaolin. Finally, seismic refraction may be very useful in studying the kaolin and its downward transition to fresh rock.

REFERENCES

Beltrame, R.J., Chandler, V.W., and Gulbranson, B.L., 1982, Geophysical investigation of the Cedar Mountain Complex, Redwood County, Minnesota: Minn. Geol. Survey, Rept. of Inv. 27, 20 p.

Davis, P.A., 1979, Interpretation of resistivity sounding data: computer programs for solutions to the forward and inverse problems: Minn. Geol. Survey, Inf. Circ. 17, 23 p.

Ervin, C.P., Ikola, R.J., and McGinnis, L.D., 1980, Simple Bouguer gravity map of Minnesota, New Ulm sheet: Minn. Geol. Survey, Misc. Map Series M-43, scale 1:250,000.

Fogelson, D.E., 1956, A gravity survey of a portion of the Redwood Falls area: Unpubl. M.S. thesis, University of Minnesota.

Grant, J.A., 1972, Minnesota River Valley, southeastern Minnesota, *in* Sims, P.K., and Morey, G.B., eds., Geology of Minnesota: A centennial volume: Minn. Geol. Survey, pp. 177-196.

Heine, J., Zanko, L.M., and Hauck, S.A., in prep., Geological, geochemical, and physical characteristics of residual and secondary kaolinitic clays in Minnesota: Natural Resources Research Institute, Tech. Rept., NRRI/GMIN-TR-89-12B.

Mooney, H.M., 1980, Handbook of engineering geophysics: Vol. 2, electrical resistivity: Bison Instrument Company, 41 p.

Orellana, E., and Mooney, H.M., 1972, Two and three layer master curves and auxiliary point diagrams for vertical electrical soundings using Wenner arrangement: Madrid, Spain, Interciencia, 43 sheets.

Parham, W.E., 1969, Clay mineralogy and geology of Minnesota's kaolin clays: Minn. Geol. Survey, Spec. Publ. SP-10, 142 p.

Appendix A

Drill Logs of Northwestern States Portland Cement Company
Drill Holes in the Munsell Beanfield

CLAY DRILL HOLE LOG SHEET

DATE 12/28/88 DRILL HOLE # Munsell #1 Page 1 of 2

FOOTAGE	ROCK/CLAY TYPE	COMMENTS
0.' TO 4.5'	Overburden	Core missing.
4.5' to 9.0'	Residual Clay (Gneiss)	65% kaolinite, 20% greyish yellow green clay, 5 GY 7/2, 15% quartz, trace iron staining. Quartz is 2 to 5 mm in diameter and angular. Gneissic textures are present but poorly preserved in the material. Minor dark yellowish brown, 10 YR 4/2, iron staining is present on some of the quartz grains and along fractures. The material is very white and weathering appears to have been moderately heavy.
9.0' to 15.6'	Residual Clay (Gneiss)	75% kaolinite, 11% 5 GY 7/2 clay, 15% quartz, 2% iron staining. Quartz is 2 to 5 mm in diameter and angular. Iron staining is pervasive. Kaolinite is white to very light grey, with clots and bands of the 5 GY 7/2 clay throughout. The banded nature in the material is similar to the relict gneissic texture seen in other areas.
15.6' to 20.3'	Residual Clay (Gneiss)	75% kaolinite, 14% 5 GY 7/2 clay, 10% quartz, 1% biotite, minor yellowish grey iron staining, 5Y 7/2. Iron staining decreases downward. Kaolinite relicts feldspar grains in part. These grains break down to a fine powder when under slight pressure. The 5 GY 7/2 clay occurs as clots with biotite associated with these clots. The matrix is kaolinite.
20.3' to 30.1'	Residual Clay (Gneiss)	17% kaolinite, 67% 5G 4/1 dark greenish grey clay, 10% biotite, 3% feldspar, 3% quartz.

20.3' to 30.1' (cont'd)		Iron staining is not present in this interval. Biotite is associated with the 5G 4/1 clay. Kaolinite occurs as clots and bands. Quartz occurs as with the kaolinite and is angular with diameters ranging from 1 to 3 mm. Feldspars are very punky and the composition is not identifiable.
30.1' to 37.4'	Residual Clay (Gneiss)	58% kaolinite, 10% 10G 6/2 pale green clay, 20% quartz, 22% feldspar, minor biotite. Feldspar is albite in composition, 0.2 to 2.1 cm in diameter and covered with kaolinite. Most grains are punky. The 10G 6/2 clay occurs as clots and bands with biotite in this material showing relict gneissic textures. Quartz is 2 to 3 mm in diameter and angular.
37.4' to 41.0'	Residual Clay (Gneiss)	24% kaolinite, 72% 5G 4/1 clay, 8% biotite, 2% feldspar, 4% quartz. Similar to the interval from 20.3 to 30.1.

CLAY DRILL HOLE LOG SHEET

DATE 12/29/88 DRILL HOLE # Munsell #2 Page 1 of 2

FOOTAGE	ROCK/CLAY TYPE	COMMENTS
0.0' TO 8.5'	Overburden	Not sampled, no core available.
8.5' to 9.5'	Residual Clay (Gneiss)	72% kaolinite, 8% 20G 6/2 pale green clay, 15% quartz, 2% biotite, 3% 10 YR 6/6 brownish yellow iron staining. The iron staining is found along fractures and on quartz grains. The 10G 6/2 clay and biotite occur as clots and bands in a kaolinite matrix, reflecting the gneiss textures of the parent material. The 10G 6/2 clay is a mixture of kaolin, illite, and chlorite.
9.5' to 14.1'	Residual Clay (Gneiss)	55% kaolinite, 32% 10G 6/2 clay, 12% quartz, 1% biotite. Similar to the previous interval, but the 10G 6/2 is increasing with depth.
14.1' to 15.3'	Residual Clay (Gneiss)	30% kaolinite, 58% 10G 6/2 clay, 7% quartz, 5% biotite. Biotite is associated with the 10G 6/2 clay and increases in abundance with depth. Kaolinite and quartz are found as clots and bands in the 10G 6/2 matrix and relict the original gneissic texture in the parent rock. Some of the kaolinite also relicts feldspar grains.

15.3' to 24.4'	Residual Clay (Gneiss)	42% kaolinite, 20% 10G 6/2 clay, 17% quartz, 18% feldspar, 3% biotite. Feldspar ranges in diameter from 0.2 to 1.3 cm. It is punky near the top of the interval but becomes less weathered with depth. The composition is albite and is sometimes found with graphic intergrowths of quartz. Some of the larger albite is associated with porphyritic dikes of material occurring at 17.2 to 17.5, 18.7 to 18.8, 22.1 to 22.5 and 24.1

DRILL HOLE # Munsell #2 Page 2 of 2

15.3' to 24.4' (cont'd)		to 24.2. Quartz is angular and 0.2 to 1.1 cm in diameter, with the largest grains being associated with the above mentioned porphyritic dikes. The clays show textures and relationships previously described in the interval from 8.5 to 9.5. The clays are not common in the dike material.
24.4' to 26.6'	Residual Clay (Gneiss)	30% kaolinite, 51% 10G 6/2 clay, 7% quartz, 7% feldspar, 5% biotite. Similar to the interval from 14.1 to 15.3 with the addition of albite found in the kaolinite bands.
26.6' to 33.5'	Residual Clay (Gneiss)	35% kaolinite, 25% 10G 6/2 clay, 12% quartz, 25% feldspar, 3% biotite. Similar to the interval from 15.3 to 24.4. Feldspar ranges in diameter form 0.2 to 1.6 cm, quartz from 0.2 to 1.1 cm. The largest quartz and feldspar is associated with porphyritic dikes occurring at 26.2 to 26.5, 27.1 to 27.2, 30.1 to 30.3, and 33.1 to 33.2. The clay areas have relict gneissic textures described previously.

CLAY DRILL HOLE LOG SHEET

DATE 12/29/88 DRILL HOLE # Munsell #3 Page 1 of 2

FOOTAGE	ROCK/CLAY TYPE	COMMENTS
0.0' TO 4.5'	Overburden	Not sampled, no core available.
4.5' to 5.1'	Secondary Clay (Recent)	88% 5Y 7/1 light grey clay, 3% quartz, 7% feldspar, 2% 10 YR 6/6 brownish yellow iron staining. Quartz and feldspar are both 2 to 4 mm in diameter and subangular to subrounded. Quartz and feldspar from crude clay-supported beds, 1 to 5 cm, and are interbedded with clay beds 3 to 10 cm thick. The lower contact is sharp with the residual clay. The upper was not sampled.
5.1' to 6.2'	Residual Clay (Gneiss)	60% kaolinite, 21% feldspar, 17% quartz, 2% 5 GY 6/1 greyish green clay, trace biotite. Banding is noted in the kaolin and 5 GY 6/1, and represents relict gneissic textures. Quartz and feldspar are 2 to 4 mm on diameter and both ar angular. Contacts between the upper and lower units are sharp. Biotite is associated with the 5 GY 6/1 clay, quartz; feldspar is associated with kaolin.
6.2' to 8.5'	Residual Clay (Mafic dike)	70% 5 Y 6/4 pale olive clay, 25% biotite, 3% 2.5Y 6/6 olive yellow iron staining, 2% kaolinite, minor quartz, feldspar and magnetite. The interval is composed of massive 5Y 6/4 clay with a homogeneous mixture of biotite and iron staining. Kaolin, quartz and feldspar are found in the interval from 7.5 to 7.9 and are a weathered gneiss xenolith.

8.5' to 9.1'	Residual Clay (Mafic dike)	80% 5 GY 6/1 greenish grey clay, 20% biotite, minor magnetite.

DRILL HOLE # Munsell #3 Page 2 of 2

8.5' to 9.1' (cont'd)		Similar to previous interval, but lacks the iron staining.
9.1' to 9.8'	Residual Clay (Gneiss)	20% kaolinite, 65% 5 GY 6/1 clay, 4% Quartz, 1% feldspar, minor biotite, and 10 YR 6/6 brownish yellow iron staining. Quartz and feldspar range in diameter from 2 to 7 mm except in the interval from 12.5 to 12.9 where they may reach 1.3 cm in size. This interval is similar to felsic dikes seen in the area. Kaolinite, quartz and feldspar form discrete bands in the mixture of the 5 GY 6/1 clay and biotite and show relict gneissic textures.
14.2' to 15.3'	Residual Clay (Gneiss)	29% kaolinite, 40% 5 GY 6/1 clay, 15% quartz, 25% feldspar, and 1% biotite. Similar to the last interval but not as well weathered. The core is in very poor condition and textures are not observed.
15.3' to 17.2'	Residual Clay (Mafic dike)	83% 5 GY 6/1 clay, 13% biotite, 2% kaolinite, 2% quartz, minor feldspar and magnetite. Similar to the interval from 8.5 to 9.1. Quartz, kaolinite and feldspar are found in xenolith near the top of the interval.
17.2' to 47.5'	Residual Clay (Gneiss)	20% kaolinite, 45% 5G 6/1 clay, 20% feldspar, 12% quartz, 3% biotite. Relict gneissic textures are observed as banding between the 5G 6/1 clay with biotite, and the kaolinite with quartz and feldspar. Quartz ranges from 2 to 7 mm in diameter and is angular in shape. Feldspar ranges in diameter from 0.2 to 1.1 cm and angular. The coarsest quartz and feldspar are found in dike, at 26.9 to 27.1, 27.4 to 27.6 and 42.3 to 42.4.

CLAY DRILL HOLE LOG SHEET

DATE 12/29/88 DRILL HOLE # Munsell #4 Page 1 of 2

FOOTAGE	ROCK/CLAY TYPE	COMMENTS
0.0' to 8.0'	Overburden	No samples available.
8.0' to 9.4'	Residual Clay (Gneiss) ((88-184))	35% kaolinite, 45% 5G 6/1 greyish green clay, 12% feldspar, 6% quartz, 1% biotite, 1% 10 YR 6/4 light yellowish brown iron staining. Gneissic textures are poorly preserved by banding between the two clay types, and overprinted by iron staining. Quartz and feldspar are associated with the kaolinite. Quartz is 2 to 3 mm in diameter and angular, feldspar is 2 to 5 mm and albite in composition. Biotite is associated with the 5G 6/1 clay. The 5G 6/1 clay is a mixture of chlorite, illite and kaolinite.
9.4' to 10.1'	Residual Clay (Mafic dike)	6% kaolinite, 83% 5G 4/1 dark greenish grey clay, 10% feldspar, 1% quartz, minor 10YR 6/4 iron staining. Quartz, feldspar and kaolinite appear to be xenoliths in a weathered mafic dike composed of a massive 5G 4/1 clay, which is composed dominantly of chlorite.
10.1' to 12.8'	Residual Clay (Gneiss)	28% kaolinite, 32% 5G 6/1 clay, 25% feldspar, 12% quartz, 3% biotite. Similar to the interval from 8.0 to 9.4 without the iron staining.
12.8' to 15.7'	Residual Clay (Gneiss and small mafic dikes)	25% kaolinite, 52% 5G 4/1 clay, 12% feldspar, 8% quartz, 3% biotite. Similar to the last interval, with three small weathered mafic dikes composed of massive 5G 4/1 clay occurring at 12.8 to 13.1, 13.4 to 13.6 and 14.2 to 14.3.

15.7' to 23.4'	Residual Clay (Mafic dike)	78% 5G 4/1 clay, 17% feldspar, 2% kaolin, 3% biotite. Feldspar shows a relict subophytic texture in the 5G 4/1 clay matrix, is albite in composition, and has a minor amount of kaolinite weathering along fractures and on crystal faces. Two weathered xenoliths showing relict gneissic textures occur at 20.7 to 21.1 and 21.3 to 21.6.
23.4' to 26.5'	Residual Clay (Gneiss)	20% kaolinite, 53% 5G 4/1 clay, 20% feldspar, 6% quartz, 1% biotite. Feldspar is 0.2 to 1.3 cm in diameter, quartz is 2 to 5 mm and angular. Textures and relationship of the minerals is similar to that found in the interval from 8.0 to 9.4.

CLAY DRILL HOLE LOG SHEET

DATE 12/29/88 DRILL HOLE # Munsell #5 Page 1 of 1

FOOTAGE	ROCK/CLAY TYPE	COMMENTS
0.0' TO 17.0'	Overburden	No sample available.
17.0' to 19.5'	Secondary Clay ((88-186))	49% kaolinite, 20% 5Y 6/1 grey clay, 19% feldspar, 12% quartz, 1% 10 YR 6/4 light yellowish brown iron staining. Quartz and feldspar form a crude bedding. Quartz is 2 to 4 mm in diameter and subangular. Feldspar is 2 to 5 mm in diameter and shows signs of rounding and abrasion. Iron staining is strongest in these beds. The quartz and feldspar are clay supported and separated by clay beds 2 to 10 cm in thickness. This is most likely a recent deposit.
19.5' to 42.7'	Residual Clay (Gneiss) ((88-187))	61% kaolinite, 15% 5Y 6/1 clay, 17% feldspar, 2% quartz. Quartz and feldspar are both angular and range from 2 to 5 mm in diameter. Feldspar is albite in composition. Relict gneissic textures are observed in the banding of the two clay types. Quartz and feldspar increase with depth.
42.7' to 51.1'	Residual Clay (Gneiss) ((88-188))	21% kaolinite, 37% 5G 7/1 light greenish grey clay, 32% feldspar, 10% quartz. Similar to the last interval. Quartz and feldspar are 2 to 7 mm in diameter and increase with depth.
51.1' to 54.5'	Residual Clay (Gneiss) ((88-189))	32% kaolinite, 21% 5G 7/1 clay, 33% feldspar, 14% quartz. Similar to the previous interval. Quartz and feldspar range in diameter from 2 to 8 mm, and appear fresher with depth.

CLAY DRILL HOLE LOG SHEET

DATE 12/27/88 DRILL HOLE # Munsell #7 Page 1 of 2

FOOTAGE	ROCK/CLAY TYPE	COMMENTS
0.0' to 3.5'	Overburden	No core available.
3.5' to 4.3'	Claying Gravel	Clasts are fresh quartz, feldspar, and gneiss, similar to material found in outcrop. The matrix is a sandy clay. The unit is clast supported and 10 YR 6/6 brownish yellow in color.
4.3' to 4.5'	Secondary Clay	74% kaolinite, 20% weathered feldspar, 6% quartz, and minor iron staining. Quartz and feldspar are supported in a clay matrix of kaolinite. Both are subangular, showing some degree of weathering as well as minor mechanical abrasion. Quartz ranges from 2 to 7 mm in diameter, and felspar 0.2 to 1.3 cm. Quartz and feldspar delineate crude bedding in the material which is enhanced by minor iron staining in these areas.
4.5' to 5.2'	Residual Clay (Gneiss)	25% kaolinite, 63% 5 GY 7/2 greyish yellow green clay, 3% biotite, 4% quartz, minor biotite and 5 Y 8/4 greyish yellow iron staining. Quartz and kaolinite occur as bands and clots in a mixture of the 5 GY 7/2 clay and biotite, replacing gneissic textures. Kaolinite also replaces feldspar grains, and increases in abundance downward.
5.2' to 9.3'	Residual Clay (Gneiss)	52% kaolinite, 40% 5 GY 7/2 clay, 2% muscovite, 7% quartz, minor biotite. Similar to the previous interval, but with more kaolinite present. Relict gneissic textures are observed between the two clays.

9.3' to 10.7'	Residual Clay (Gneiss)	15% kaolinite, 70% 5 GY 7/2 clay, 5% feldspar, 7% quartz, 2% muscovite, 1% biotite, minor iron staining. Iron staining commonly found as a coating on quartz and feldspar grains. Feldspar is 2 to 3 mm in diameter and blocky. Quartz is angular and similar in size. Feldspar increases with depth. Quartz and feldspar are associated with kaolinite as bands and clots in the 5 GY 7/2 clay reflecting relict gneissic textures.
10.7' to 14.2'	Residual Clay (Gneissic)	30% kaolinite, 42% 5G 6/1 greenish grey clay, 20% feldspar, 5% quartz, 2% biotite, 1% muscovite. Feldspar is 0.2 to 2.0 cm in diameter and only weathered on the surface. Quartz is 2 to 3 mm. The core is broken up and no pieces large enough to show textures remain. It is probable that this interval is similar to others observed in the area where felsic dikes cut the gneiss.
14.2' to 34.5'	Residual Clay (Gneiss)	25% kaolin, 45% 5G 6/1 clay, 20% feldspar, 3% biotite, 2% muscovite, 5% quartz. Similar to the last interval. Feldspar and quartz form some graphic intergrowths, and feldspar grains appear less weathered with depth.

CLAY DRILL HOLE LOG SHEET

DATE 1/4/89 DRILL HOLE # Munsell #8 Page 1 of 1

FOOTAGE	ROCK/CLAY TYPE	COMMENTS
0.0' TO 7.5'	Overburden	No sample present.
7.5' to 9.1'	Residual Clay (Gneiss) ((88-190))	60% kaolinite, 10% 5B 7/1 light bluish-grey clay, 12% quartz, 11% feldspar, 1% biotite, 1% 10 YR 8/4 very pale brown iron staining. Quartz and feldspar are 2 to 5 mm in diameter and associated with the kaolinite. Biotite is associated with the 5B 7/1 clay. Relict gneiss textures are inferred by the bonding of the two clay types.
9.1' to 17.3'	Residual Clay (Gneiss) ((88-191))	55% kaolinite, 6% 5B 7/1 clay, 14% quartz, 24% feldspar, 1% biotite. Similar to the last interval. Quartz and feldspar increase with depth. Feldspar is 0.2 to 1.3 cm in diameter, quartz 2 to 6 mm.
17.3' to 26.5'	Residual Clay (Gneiss) ((88-192))	47% kaolinite, 6% 5B light bluish-grey clay, 31% feldspar, 15% quartz, 1% biotite. Similar to the last interval. Quartz and feldspar are fresher looking and beginning to form definite bands of grus which are 0.5 to 1.1 cm wide, with a kaolinite matrix. Core is poorly preserved in these areas. Gneissic textures are seen in the more clay-rich areas.

Appendix B

Resistivity Data--Field Notes

Spread 1a east-west

Spread 1b north-south

a (m)	ρa LL	ρa LR	ρa W	ρa LL	ρa LR	ρa W	Avg. ρa W
.91	204	160	186	217	175	198	192
1.52	198	179	198	188	179	191	194
2.44	201	207	205	201	198	201	203
3.66	176	197	187	239	174	209	198
7.62	113	149	133	180	113	149	141
15.24	118	123	122	120	108	116	119
30.48	144	170	161	163	145	156	159
45.72	190	229	214	216	206	214	214
60.96	250	288	272	273	251	266	269
91.44	404	397	407	347	309	336	372

Spread 2

a (m)	ρa LL	ρa LR	ρa W
0.91	122	135	129
1.52	136	155	147
2.44	155	150	153
3.66	129	119	126
7.62	66	96	85
15.24	63	109	87
30.48	92	171	130
45.72	119	234	180
60.96	191	301	247
91.44	377	486	382

Spread 3

a (m)	ρa LL	ρa LR	ρa W	Cross-check ρa W
0.91	30	39	35	
1.52	45	48	47	
2.44	55	60	59	
3.66	71	79	77	83
7.62	108	107	110	
15.24	158	137	149	

Spread 4b (east-west)				Spread 4a (north-south)			
a (m)	ρa LL	ρa LR	ρa W	ρa LL	ρa LR	ρa W	Avg. ρa W
.91	100	100	108	91	97	98	103
1.52	122	123	123	135	133	134	129
2.44	158	160	160	162	165	165	162
3.66	179	179	180	187	185	187	184
7.62	142	155	152	166	168	174	163
15.24	104	119	112	125	125	125	119
30.48	122	128	126	128	122	128	127
45.72	--	--	--	165	165	168	168
60.96	219	256	239	220	220	218	229
91.44	329	329	346	329	347	334	340

Spread 5

a (m)	ρa LL	ρa LR	ρa W	Cross-check ρa W
0.91	101	155	129	--
1.52	106	135	122	--
2.44	89	108	100	--
3.66	73	87	82	--
7.62	59	79	70	--
15.24	67	76	72	--
30.48	91	104	101	112
45.72	128	146	139	--
60.96	171	183	181	--

Spread 6

a (m)	ρa LL	ρa LR	ρa W	Cross-check ρa W
0.91	229	249	242	
1.52	280	249	265	
2.44	322	273	298	
3.66	305	267	288	
7.62	184	171	180	
15.24	125	158	141	127
30.48	122	165	145	170
45.72	183	238	215	221
60.96	256	328	293	
91.44	402	512	464	

Spread 7

a (m)	ρa LL	ρa LR	ρa W	Cross-check ρa W
0.91	33	35	34	--
1.52	50	52	52	--
2.44	74	71	74	--
3.66	100	83	91	--
7.62	104	67	85	--
15.24	76	71	74	--
30.48	98	98	98	100
45.72	137	137	137	--
60.96	183	183	187	--
91.44	293	311	305	--

Spread 8

a (m)	ρa LL	ρa LR	ρa W	Cross-check ρa W
0.91	173	218	855	--
1.52	307	423	707	875
2.44	195	249	466	--
3.66	114	208	236	--
7.62	198	41	233	--

Spread 9

a (m)	ρa LL	ρa LR	ρa W
0.91	--	137	176
1.52	144	116	125
2.44	131	106	119
3.66	120	92	120
7.62	88	104	105

Spread 10

a (m)	ρa LL	ρa LR	ρa W
0.91	45	39	43
1.52	40	40	41
2.44	53	48	52
3.66	62	40	52
7.62	56	49	54
15.24	--	--	61

Spread 11

a (m)	ρa LL	ρa LR	ρa W
0.91	51	80	66
1.52	37	68	54
2.44	35	59	48
3.66	42	53	50
7.62	45	56	50
15.24	48	61	55

Spread 12

a (m)	ρa LL	ρa LR	ρa W
0.91	17	29	24
1.52	21	30	26
2.44	25	35	30

Spread 13

a (m)	ρa LL	ρa LR	ρa W
0.91	79	73	82
1.52	46	47	46
2.44	27	33	30
3.66	27	27	26
7.62	29	35	32
15.24	40	37	43

Spread 14

a (m)	ρa LL	ρa LR	ρa W
0.91	33	36	35
1.52	27	26	27
2.44	22	20	21
3.66	20	17	19
7.62	23	20	22
15.24	30	27	29

a = spacing (m.)
ρa LL = Lee left (ohm m.)
ρa LR = Lee right (ohm m.)
ρa W = Wenner (ohm m.)

Appendix C

Gravity Data Reduced to Sea Level Datum and 2.67 gm/cc

Station	Bouguer Anomaly (milligals)	UTM Easting[1]	UTM Northing[2]
004N	-41.13	971.0	8160.0
003N	-41.14	970.0	8129.0
002N	-41.06	970.0	8099.0
001N	-41.36	970.0	8068.0
00BL	-41.61	970.0	8038.0
001S	-41.76	969.0	8006.0
002S	-41.99	969.0	7975.0
003S	-42.07	970.0	7915.0
004S	-42.09	970.0	7885.0
005S	-42.05	970.0	7823.0
007S	-41.94	970.0	7823.0
009S	-41.92	969.0	7763.0
0011S	-41.99	969.0	7702.0
0013S	-42.02	969.0	7646.0
0015S	-41.97	969.0	7580.0
0017S	-42.29	968.0	7520.0
0019S	-42.50	969.0	7459.0
2W20S	-42.53	945.0	7430.0
2W18S	-42.29	940.0	7491.0
2W16S	-42.14	937.0	7552.0
2W14S	-42.04	934.0	7612.0
2W12S	-42.13	931.0	7672.0
2W10S	-42.13	925.0	7734.0
2W08S	-41.98	922.0	7793.0
2W06S	-41.89	918.0	7854.0
2W04S	-41.97	915.0	7915.0
2W02S	-41.94	912.0	7975.0
2WBL	-41.60	910.0	8038.0
2W02N	-41.37	906.0	8097.0
2E03N	-41.26	1028.0	8130.0
2E01N	-41.23	1029.0	8069.0
2E01S	-41.74	1032.0	8007.0
2E03S	-42.08	1034.0	7945.0
2E06S	-42.07	1038.0	7854.0
2E09S	-41.98	1040.0	7763.0
2E12S	-42.03	1045.0	7671.0
2E15S	-42.01	1049.0	7581.0
2E18S	-42.19	1053.0	7491.0
2E21S	-42.42	1056.0	7401.0
4E18S	-42.05	1142.0	7492.0
4E15S	-41.98	1133.0	7583.0
4E12S	-41.97	1124.0	7676.0
4E09S	-41.77	1116.0	7763.0
4E06S	-41.99	1108.0	7853.0
4E03S	-41.84	1099.0	7945.0
4EBL	-41.16	1092.0	8036.0

[1]minus 350,000

[2]minus 4,920,000

Appendix D

Magnetic Data Diurnally Corrected

5/23/90

LOOPALL2 is a listing of the data used to produce the magnetic map for the Munsell kaolin project. The magnetic values have been corrected for diurnal variation. One thousand meters were subtracted from the eastings after a surveying error was reported in establishing the original UTM's.

Station Name	Magnetic Value[1]	UTM Easting[2]	UTM Northing[3]
8+00N	1153.	972.0	8283.0
7+80N	1145.	971.8	8276.8
7+60N	1141.	971.6	8270.6
7+40N	1130.	971.4	8264.4
7+20N	1148.	971.2	8258.2
7+00N	1131.	971.0	8252.0
6+80N	1130.	970.8	8246.0
6+60N	1113.	970.6	8240.0
6+40N	1099.	970.4	8234.0
6+20N	1085.	970.2	8228.0
6+00N	1073.	970.0	8222.0
5+80N	1065.	970.0	8215.8
5+60N	1031.	970.0	8209.6
5+40N	925.	970.0	8203.4
5+20N	886.	970.0	8197.2
5+00N	897.	970.0	8191.0
4+80N	881.	970.2	8184.8
4+60N	937.	970.4	8178.6
4+40N	956.	970.6	8172.4
4+20N	976.	970.8	8166.2
4+00N	996.	971.0	8160.0
3+80N	1011.	970.8	8153.8
3+60N	1022.	970.6	8147.6
3+40N	1028.	970.4	8141.4
3+20N	1047.	970.2	8135.2
3+00N	1048.	970.0	8129.0
2+80N	1020.	970.0	8123.0
2+60N	984.	970.0	8117.0
2+40N	986.	970.0	8111.0
2+20N	1021.	970.0	8105.0
2+00N	1025.	970.0	8099.0
1+80N	1068.	970.0	8092.8
1+60N	1106.	970.0	8086.6
1+40N	1067.	970.0	8080.4
1+20N	1035.	970.0	8074.2
1+00N	999.	970.0	8068.0
0+80N	1005.	970.0	8062.0

Station Name	Magnetic Value[1]	UTM Easting[2]	UTM Northing[3]
0+60N	1051.	970.0	8056.0
0+40N	1150.	970.0	8050.0
0+20N	1114.	970.0	8044.0
0+00N	1098.	970.0	8038.0
0+20S	1092.	969.8	8031.6
0+40S	1117.	969.6	8025.2
0+60S	1198.	969.4	8018.8
0+8OS	1227.	969.2	8012.4
1+00S	1234.	969.0	8006.0
1+20S	1206.	969.0	7999.8
1+40S	1179.	969.0	7993.6
1+60S	1150.	969.0	7987.4
1+80S	1144.	969.0	7981.2
2+00S	1135.	969.0	7975.0
2+20S	1127.	969.2	7969.0
2+40S	1124.	969.4	7963.0
2+60S	1118.	969.6	7957.0
2+80S	1112.	969.8	7951.0
3+00S	1115.	970.0	7945.0
3+20S	1109.	970.0	7939.0
3+40S	1105.	970.0	7933.0
3+60S	1101.	970.0	7927.0
3+80S	1098.	970.0	7921.0
4+00S	1099.	970.0	7915.0
4+20S	1097.	970.0	7909.0
4+40S	1097.	970.0	7903.0
4+60S	1096.	970.0	7897.0
4+80S	1094.	970.0	7891.0
5+00S	1092.	970.0	7885.0
5+20S	1091.	969.8	7878.8
5+40S	1091.	969.6	7872.6
5+60S	1090.	969.4	7866.4
5+80S	1087.	969.2	7860.2
6+00S	1086.	969.0	7854.0
6+20S	1087.	969.2	7847.8
6+40S	1086.	969.4	7841.6
6+60S	1084.	969.6	7835.4
6+80S	1088.	969.8	7829.2
7+00S	1091.	970.0	7823.0
7+20S	1089.	969.6	7817.2
7+40S	1086.	969.2	7811.4
7+60S	1086.	968.8	7805.6
7+80S	1083.	968.4	7799.8
8+00S	1079.	968.0	7794.0
8+20S	1075.	968.2	7787.8

Station Name	Magnetic Value[1]	UTM Easting[2]	UTM Northing[3]
8+40S	1074.	968.4	7781.6
8+60S	1083.	968.6	7775.4
8+80S	1082.	968.8	7769.2
9+00S	1081.	969.0	7763.0
9+20S	1087.	969.2	7756.8
9+40S	1090.	969.4	7750.6
9+60S	1079.	969.6	7744.4
9+8OS	1080.	969.8	7738.2
10+00S	1083.	970.0	7732.0
10+20S	1082.	969.8	7726.0
10+40S	1086.	969.6	7720.0
10+60S	1079.	969.4	7714.0
10+80S	1068.	969.2	7708.0
11+00S	1073.	969.0	7702.0
11+20S	1074.	969.0	7695.8
11+40S	1073.	969.0	7689.6
11+60S	1073.	969.0	7683.4
11+80S	1076.	969.0	7677.2
12+00S	1076.	969.0	7671.0
12+20S	1076.	969.0	7666.0
12+40S	1075.	969.0	7661.0
12+60S	1082.	969.0	7656.0
12+80S	1083.	969.0	7651.0
13+00S	1092.	969.0	7646.0
13+20S	1084.	969.0	7639.0
13+40S	1081.	969.0	7632.0
13+60S	1079.	969.0	7625.0
13+80S	1078.	969.0	7618.0
14+00S	1078.	969.0	7611.0
14+20S	1073.	969.0	7604.8
14+40S	1066.	969.0	7598.6
14+60S	1063.	969.0	7592.4
14+80S	1059.	969.0	7586.2
15+00S	1055.	969.0	7580.0
15+20S	1052.	969.0	7574.4
15+40S	1047.	969.0	7568.8
15+60S	1044.	969.0	7563.2
15+80S	1041.	969.0	7557.6
16+00S	1041.	969.0	7552.0
16+20S	1040.	968.8	7545.6
16+40S	1037.	968.6	7539.2
16+60S	1033.	968.4	7532.8
16+80S	1030.	968.2	7526.4
17+00S	1030.	968.0	7520.0
17+20S	1034.	968.2	7513.8

Station Name	Magnetic Value[1]	UTM Easting[2]	UTM Northing[3]
17+40S	1060.	968.4	7507.6
17+60S	1083.	968.6	7501.4
17+80S	1076.	968.8	7495.2
18+00S	1062.	969.0	7489.0
18+20S	1054.	969.0	7483.0
18+40S	1052.	969.0	7477.0
18+60S	1053.	969.0	7471.0
18+80S	1055.	969.0	7465.0
19+00S	1056.	969.0	7459.0
19+20S	1055.	969.0	7453.0
19+40S	1056.	969.0	7447.0
19+60S	1056.	969.0	7441.0
19+80S	1057.	969.0	7435.0
20+00S	1062.	969.0	7429.0
8+00N	1178.	895.0	8281.0
7+80N	1171.	895.4	8274.8
7+60N	1163.	895.8	8268.6
7+40N	1151.	896.2	8262.4
7+20N	1138.	896.6	8256.2
7+00N	1125.	897.0	8250.0
6+80N	1109.	897.4	8243.8
6+60N	1103.	897.8	8237.6
6+40N	1088.	898.2	8231.4
6+20N	1043.	898.6	8225.2
6+00N	902.	899.0	8219.0
5+80N	751.	899.4	8214.0
5+60N	60.	899.8	8209.0
5+40N	1226.	900.2	8204.0
5+20N	2053.	900.6	8199.0
5+00N	1121.	901.0	8194.0
4+80N	991.	901.4	8187.2
4+60N	956.	901.8	8180.4
4+40N	991.	902.2	8173.6
4+20N	999.	902.6	8166.8
4+00N	1016.	903.0	8160.0
3+80N	1037.	903.4	8153.8
3+60N	1033.	903.8	8147.6
3+40N	1008.	904.2	8141.4
3+20N	1010.	904.6	8135.2
3+00N	983.	905.0	8129.0
2+80N	1079.	905.2	8122.6
2+60N	1157.	905.4	8116.2
2+40N	1147.	905.6	8109.8
2+20N	1183.	905.8	8103.4
2+00N	1168.	906.0	8097.0

Station Name	Magnetic Value[1]	UTM Easting[2]	UTM Northing[3]
1+80N	1104.	906.0	8091.8
1+60N	1093.	906.0	8086.6
1+40N	1081.	906.0	8081.4
1+20N	1038.	906.0	8076.2
1+00N	1039.	906.0	8071.0
0+80N	1031.	906.8	8064.4
0+60N	1053.	907.6	8057.8
0+40N	1096.	908.4	8051.2
0+20N	1108.	909.2	8044.6
0+00N	1110.	910.0	8038.0
0+20S	1106.	910.2	8031.4
0+40S	1111.	910.4	8024.8
0+60S	1105.	910.6	8018.2
0+8OS	1119.	910.8	8011.6
1+00S	1128.	911.0	8005.0
1+50S	1136.	911.5	7990.0
2+00S	1136.	912.0	7975.0
2+50S	1124.	912.5	7961.0
3+00S	1111.	913.0	7947.0
3+00S	1111.	913.0	7947.0
3+50S	1258.	914.0	7931.0
3+80S	1483.	914.6	7921.4
4+00S	1492.	915.0	7915.0
4+20S	1391.	915.4	7909.0
4+40S	1281.	915.8	7903.0
4+60S	1201.	916.2	7897.0
4+80S	1163.	916.6	7891.0
5+00S	1141.	917.0	7885.0
5+50S	1108.	917.5	7869.5
6+00S	1096.	918.0	7854.0
6+50S	1089.	919.0	7839.0
7+00S	1093.	920.0	7824.0
7+50S	1102.	921.0	7808.5
8+00S	1120.	922.0	7793.0
8+20S	1130.	922.4	7787.2
8+40S	1118.	922.8	7781.4
8+60S	1117.	923.2	7775.6
8+80S	1112.	923.6	7769.8
9+00S	1106.	924.0	7764.0
9+50S	1097.	924.5	7749.0
10+00S	1093.	925.0	7734.0
10+50S	1081.	926.5	7718.0
11+00S	1081.	928.0	7702.0
11+50S	1084.	929.5	7687.0
12+00S	1083.	931.0	7672.0

Station Name	Magnetic Value[1]	UTM Easting[2]	UTM Northing[3]
12+50S	1080.	931.5	7657.0
13+00S	1077.	932.0	7642.0
13+50S	1070.	933.0	7627.0
14+00S	1063.	934.0	7612.0
14+50S	1056.	934.5	7597.0
15+00S	1047.	935.0	7582.0
15+50S	1043.	936.0	7567.0
16+00S	1040.	937.0	7552.0
16+50S	1038.	938.0	7536.5
17+00S	1060.	939.0	7521.0
17+20S	1070.	939.2	7515.0
17+40S	1070.	939.4	7509.0
17+60S	1060.	939.6	7503.0
17+80S	1049.	939.8	7497.0
18+00S	1043.	940.0	7491.0
18+50S	1042.	941.0	7475.5
19+00S	1049.	942.0	7460.0
19+50S	1054.	943.5	7445.0
20+00S	1056.	945.0	7430.0
21+00S	1075.	1056.0	7401.0
20+50S	1076.	1055.5	7414.5
20+00S	1073.	1055.0	7428.0
19+50S	1074.	1054.0	7443.5
19+00S	1083.	1053.0	7459.0
18+50S	1107.	1053.0	7475.0
18+25S	1083.	1053.0	7483.0
18+00S	1055.	1053.0	7491.0
17+80S	1046.	1052.8	7497.0
17+60S	1039.	1052.6	7503.0
17+40S	1036.	1052.4	7509.0
17+20S	1037.	1052.2	7515.0
17+00S	1038.	1052.0	7521.0
16+50S	1041.	1051.0	7535.5
16+00S	1042.	1050.0	7550.0
15+50S	1050.	1049.5	7565.5
15+00S	1053.	1049.0	7581.0
14+50S	1058.	1048.0	7596.0
14+00S	1060.	1047.0	7611.0
13+50S	1066.	1046.5	7626.5
13+00S	1072.	1046.0	7642.0
12+50S	1084.	1045.5	7656.5
12+00S	1084.	1045.0	7671.0
11+50S	1081.	1044.5	7686.5
11+00S	1079.	1044.0	7702.0
10+50S	1079.	1044.0	7717.0

Station Name	Magnetic Value[1]	UTM Easting[2]	UTM Northing[3]
10+00S	1097.	1044.0	7732.0
0+00N	1320.	1031.0	8037.0
0+20S	1076.	1031.2	8031.0
0+40S	1081.	1031.4	8025.0
0+60S	1079.	1031.6	8019.0
0+80S	1082.	1031.8	8013.0
1+00S	1084.	1032.0	8007.0
1+20S	1084.	1032.0	8000.2
1+40S	1084.	1032.0	7993.4
1+60S	1085.	1032.0	7986.6
1+80S	1089.	1032.0	7979.8
2+00S	1095.	1032.0	7973.0
2+20S	1108.	1032.4	7967.4
2+40S	1097.	1032.8	7961.8
2+60S	1093.	1033.2	7956.2
2+80S	1092.	1033.6	7950.6
3+00S	1092.	1034.0	7945.0
3+50S	1085.	1034.5	7930.0
4+00S	1078.	1035.0	7915.0
4+50S	1075.	1036.0	7899.5
5+00S	1075.	1037.0	7884.0
5+50S	1072.	1037.5	7869.0
6+00S	1071.	1038.0	7854.0
6+50S	1070.	1038.0	7840.0
7+00S	1072.	1038.0	7826.0
7+50S	1073.	1038.5	7809.5
8+00S	1072.	1039.0	7793.0
8+50S	1079.	1039.5	7778.0
9+00S	1086.	1040.0	7763.0
9+50S	1090.	1042.0	7747.5
10+00S	1098.	1044.0	7732.0
19+00S	1075.	1143.0	7462.0
18+50S	1068.	1142.5	7477.0
18+00S	1078.	1142.0	7492.0
17+50S	1090.	1139.5	7507.5
17+00S	1089.	1137.0	7523.0
16+50S	1085.	1136.0	7538.0
16+00S	1084.	1135.0	7553.0
15+50S	1080.	1134.0	7568.0
15+00S	1072.	1133.0	7583.0
14+50S	1068.	1131.0	7599.0
14+00S	1055.	1129.0	7615.0
13+75S	1063.	1128.3	7622.5
13+50S	1071.	1127.5	7630.0
13+00S	1081.	1126.0	7645.0

Station Name	Magnetic Value[1]	UTM Easting[2]	UTM Northing[3]
12+50S	1091.	1125.0	7660.5
12+00S	1093.	1124.0	7676.0
11+50S	1092.	1122.5	7691.0
11+00S	1094.	1121.0	7706.0
10+50S	1100.	1119.5	7721.5
10+00S	1110.	1118.0	7737.0
9+50S	1106.	1117.0	7750.0
9+00S	1094.	1116.0	7763.0
8+50S	1083.	1114.5	7777.5
8+00S	1074.	1113.0	7792.0
7+50S	1068.	1111.5	7807.5
7+00S	1076.	1110.0	7823.0
6+50S	1079.	1109.5	7838.0
6+00S	1087.	1108.0	7853.0
5+50S	1093.	1107.0	7868.0
5+00S	1093.	1106.0	7883.0
4+50S	1092.	1104.0	7898.5
4+00S	1090.	1102.0	7914.0
3+50S	1088.	1100.5	7929.5
3+00S	1082.	1099.0	7945.0
2+80S	1083.	1098.4	7951.2
2+60S	1085.	1097.9	7957.4
2+40S	1088.	1097.2	7963.6
2+20S	1089.	1096.6	7969.8
2+00S	1088.	1096.0	7976.0
1+80S	1087.	1095.6	7982.0
1+60S	1090.	1095.2	7988.0
1+40S	1094.	1094.8	7994.0
1+20S	1097.	1094.4	8000.0
1+00S	1133.	1094.0	8006.0
0+80S	1135.	1093.6	8012.0
0+60S	1044.	1093.2	8018.0
0+45S	1426.	1092.9	8022.3
0+20N	1073.	1030.6	8043.4
0+40N	1091.	1030.2	8049.8
0+60N	1131.	1029.8	8056.2
0+80N	1237.	1029.4	8062.6
1+00N	1254.	1029.0	8069.0
1+20N	1244.	1028.8	8075.0
1+40N	1136.	1028.6	8081.0
1+60N	967.	1028.4	8087.0
1+80N	949.	1028.2	8093.0
2+00N	964.	1028.0	8099.0
2+20N	989.	1028.0	8105.2
2+40N	982.	1028.0	8111.4

Station Name	Magnetic Value[1]	UTM Easting[2]	UTM Northing[3]
2+60N	1001.	1028.0	8117.6
2+80N	1013.	1028.0	8123.8
3+00N	1017.	1028.0	8130.0
3+20N	1015.	1027.7	8136.0
3+40N	1005.	1027.4	8142.0
3+60N	1023.	1027.1	8148.0
3+80N	1040.	1026.8	8154.0
4+00N	891.	1026.5	8160.0
4+20N	816.	1026.2	8166.0
4+40N	788.	1025.9	8172.0
4+60N	804.	1025.6	8178.0
4+8ON	856.	1025.3	8184.0
5+00N	919.	1025.0	8190.0
5+20N	936.	1024.8	8196.0
5+40N	970.	1024.6	8202.0
5+60N	1014.	1024.4	8208.0
5+80N	1045.	1024.2	8214.0
6+00N	1063.	1024.0	8220.0
6+20N	1083.	1023.8	8226.0
6+40N	1096.	1023.6	8232.0
6+60N	1092.	1023.4	8238.0
6+80N	1107.	1023.2	8244.0
7+00N	1111.	1023.0	8250.0
7+00N	1118.	1068.0	8249.0
6+80N	1114.	1068.7	8242.9
6+60N	1106.	1069.4	8236.8
6+40N	1099.	1070.1	8230.7
6+20N	1091.	1070.8	8224.6
6+00N	1086.	1071.5	8218.5
5+80N	1079.	1072.2	8212.4
5+60N	1068.	1072.9	8206.3
5+40N	1045.	1073.6	8200.2
5+20N	1032.	1074.3	8194.1
5+00N	1010.	1075.0	8188.0
4+80N	998.	1075.7	8181.9
4+60N	968.	1076.4	8175.8
7+00N	1111.	1196.0	8249.0
6+80N	1108.	1196.2	8242.8
6+60N	1101.	1196.4	8236.6
6+40N	1094.	1196.6	8230.4
6+20N	1088.	1196.8	8224.2
6+00N	1084.	1197.0	8218.0
5+80N	1079.	1197.8	8212.0
5+60N	1074.	1198.6	8206.0
5+40N	1068.	1199.4	8200.0

Station Name	Magnetic Value[1]	UTM Easting[2]	UTM Northing[3]
5+20N	1063.	1200.2	8194.0
5+00N	1060.	1201.0	8188.0
4+80N	1055.	1200.2	8182.0
4+60N	1054.	1199.4	8176.0
4+40N	1052.	1198.6	8170.0
4+20N	1050.	1197.8	8164.0
4+00N	1050.	1197.0	8158.0
3+80N	1040.	1199.0	8152.0
3+60N	1050.	1201.0	8146.0
3+40N	1048.	1203.0	8140.0
3+20N	1052.	1205.0	8134.0
3+00N	1055.	1207.0	8128.0
2+80N	1063.	1207.4	8121.8
2+60N	1071.	1207.8	8115.6
2+40N	1073.	1208.2	8109.4
2+2ON	1081.	1208.6	8103.2
2+00N	1079.	1209.0	8097.0
1+80N	1075.	1209.6	8091.0
1+60N	1056.	1210.2	8085.0
1+40N	945.	1210.8	8079.0
1+20N	764.	1211.4	8073.0
1+00N	851.	1212.0	8067.0
0+80N	996.	1212.2	8060.8
0+60N	1056.	1212.4	8054.6
0+40N	1126.	1212.6	8048.4
0+20N	1146.	1212.8	8042.2
0+00N	1050.	1213.0	8036.0
0+20S	1017.	1213.0	8030.2
0+40S	1211.	1213.0	8024.4
0+60S	1072.	1213.0	8018.6
0+80S	1051.	1213.0	8012.8
1+00S	1040.	1213.0	8007.0
1+20S	1043.	1213.8	8001.0
1+40S	1239.	1214.6	7995.0
1+60S	1039.	1215.4	7989.0
1+80S	1040.	1216.2	7983.0
2+00S	1037.	1217.0	7977.0
2+00S	1033.	1217.0	7977.0
2+20S	1029.	1217.4	7970.8
2+40S	1033.	1217.8	7964.6
2+60S	1035.	1218.2	7958.4
2+80S	1032.	1218.6	7952.6
3+00S	1035.	1219.0	7946.0
3+20S	1038.	1219.0	7940.0
3+40S	1042.	1219.0	7934.0

Station Name	Magnetic Value[1]	UTM Easting[2]	UTM Northing[3]
3+60S	1042.	1219.0	7928.0
3+80S	1044.	1219.0	7922.0
4+00S	1051.	1219.0	7916.0
4+50S	1050.	1221.0	7900.0
5+00S	1052.	1223.0	7884.0
5+50S	1054.	1224.0	7869.5
6+00S	1054.	1225.0	7855.0
6+50S	1054.	1226.0	7839.5
7+00S	1052.	1227.0	7824.0
7+50S	1053.	1227.5	7811.0
8+00S	1044.	1228.0	7798.0
8+50S	1036.	1229.5	7783.0
9+00S	1039.	1231.0	7768.0
9+50S	1049.	1231.5	7752.5
10+00S	1071.	1232.0	7737.0
10+25S	1069.	1232.8	7729.5
10+50S	1075.	1233.5	7722.0
10+75S	1083.	1234.3	7714.5
11+00S	1086.	1235.0	7707.0
11+25S	1090.	1235.3	7699.3
11+50S	1089.	1235.5	7691.5
11+75S	1091.	1235.8	7683.8
12+00S	1088.	1236.0	7676.0
12+50S	1082.	1237.0	7660.5
13+00S	1066.	1238.0	7645.0
13+50S	1056.	1239.0	7630.0
14+00S	1070.	1240.0	7615.0
14+50S	1096.	1241.0	7600.0
15+00S	1092.	1242.0	7585.0
15+00S	1076.	1177.0	7584.0
14+50S	1048.	1176.5	7599.0
14+00S	1031.	1176.0	7614.0
13+50S	1045.	1175.0	7629.5
13+00S	1074.	1174.0	7645.0
12+50S	1093.	1173.5	7660.5
12+25S	1100.	1173.3	7668.3
12+00S	1094.	1173.0	7676.0
11+75S	1095.	1172.5	7683.5
11+50S	1098.	1172.0	7691.0
11+00S	1099.	1171.0	7706.0
10+50S	1090.	1170.5	7721.0
10+00S	1090.	1170.0	7736.0
9+50S	1086.	1169.0	7751.0
9+00S	1073.	1168.0	7766.0
8+75S	1059.	1167.5	7773.8

Station Name	Magnetic Value[1]	UTM Easting[2]	UTM Northing[3]
8+50S	1049.	1167.0	7781.5
8+25S	1048.	1166.5	7789.3
8+00S	1051.	1166.0	7797.0
7+50S	1060.	1165.5	7809.5
7+00S	1069.	1165.0	7822.0
6+50S	1068.	1163.5	7838.0
6+00S	1067.	1162.0	7854.0
5+50S	1072.	1161.5	7869.0
5+00S	1059.	1161.0	7884.0
4+80S	1062.	1160.6	7890.2
4+60S	1067.	1160.2	7896.4
4+40S	1067.	1159.8	7902.6
4+20S	1073.	1159.4	7908.8
4+00S	1098.	1159.0	7915.0
3+80S	1064.	1158.6	7921.0
3+60S	1065.	1158.2	7927.0
3+40S	1070.	1157.8	7933.0
3+20S	1069.	1157.4	7939.0
3+00S	1075.	1157.0	7945.0
2+80S	1072.	1156.6	7951.2
2+60S	1059.	1156.2	7957.4
2+40S	1056.	1155.8	7963.6
2+20S	1049.	1155.4	7969.8
2+00S	1044.	1155.0	7976.0
1+80S	1040.	1154.8	7982.2
1+60S	1034.	1154.6	7988.4
1+40S	1027.	1154.4	7994.6
1+20S	1017.	1154.2	8000.8
1+00S	1004.	1154.0	8007.0
4+60N	966.	1076.4	8175.8
4+40N	935.	1077.1	8169.7
4+20N	899.	1077.8	8163.6
4+00N	822.	1078.5	8157.5
3+80N	807.	1079.2	8151.4
3+60N	811.	1079.9	8145.3
3+40N	681.	1080.6	8139.2
3+20N	1043.	1081.3	8133.1
3+00N	1042.	1082.0	8127.0
2+80N	1000.	1082.7	8121.0
2+60N	959.	1083.4	8115.0
2+40N	980.	1084.1	8109.0
2+20N	1013.	1084.8	8103.0
2+00N	1011.	1085.5	8097.0
1+80N	999.	1086.2	8091.0
1+60N	984.	1086.9	8085.0

Station Name	Magnetic Value[1]	UTM Easting[2]	UTM Northing[3]
1+40N	955.	1087.6	8079.0
1+20N	831.	1088.3	8073.0
1+00N	697.	1089.0	8067.0
0+80N	876.	1089.6	8060.8
0+60N	1038.	1090.2	8054.6
0+40N	1159.	1090.8	8048.4
0+20N	1257.	1091.4	8042.2
0+00N	1217.	1092.0	8036.0
0+20S	1147.	1092.4	8030.0
0+40S	1049.	1092.8	8024.0
0+80S	949.	1153.6	8013.0
0+60S	866.	1153.2	8019.0
0+40S	519.	1152.8	8025.0
0+20S	198.	1152.4	8031.0
0+00N	1011.	1152.0	8037.0
0+20N	1071.	1151.6	8043.0
0+40N	1036.	1151.2	8049.0
0+60N	1029.	1150.8	8055.0
0+80N	971.	1150.4	8061.0
1+00N	764.	1150.0	8067.0
1+40N	840.	1149.3	8079.2
1+60N	1015.	1148.9	8085.2
1+80N	1137.	1148.6	8091.3
2+00N	1017.	1148.2	8097.4
2+20N	944.	1147.8	8103.5
2+40N	846.	1147.5	8109.6
2+60N	781.	1147.1	8115.6
2+80N	887.	1146.8	8121.7
3+00N	920.	1146.4	8127.8
3+20N	943.	1146.0	8133.9
3+40N	966.	1145.7	8140.0
3+60N	985.	1145.3	8146.0
3+80N	1003.	1145.0	8152.1
4+00N	1013.	1144.6	8158.2
4+20N	1018.	1144.2	8164.3
4+40N	1036.	1143.9	8170.4
4+60N	1042.	1143.5	8176.4
4+80N	1049.	1143.2	8182.5
5+00N	1058.	1142.8	8188.6
5+20N	1067.	1142.4	8194.7
5+40N	1075.	1142.1	8200.8
5+60N	1084.	1141.7	8206.8
5+80N	1092.	1141.4	8212.9
6+00N	1097.	1141.0	8219.0
6+20N	1105.	1140.6	8225.2

Station Name	Magnetic Value[1]	UTM Easting[2]	UTM Northing[3]
6+40N	1109.	1140.2	8231.4
6+60N	1114.	1139.8	8237.6
6+80N	1123.	1139.4	8243.8
7+00N	1128.	1139.0	8250.0
2+00W	1091.	925.0	7734.0
1+80W	1093.	931.4	7733.7
1+60W	1093.	937.9	7733.4
1+40W	1091.	944.3	7733.1
1+20W	1089.	950.7	7732.9
1+00W	1087.	957.1	7732.6
0+20W	1088.	963.6	7732.3
0+00W	1082.	970.0	7732.0
0+20E	1076.	976.3	7732.0
0+40E	1069.	982.7	7732.0
0+60E	1067.	989.0	7732.0
0+80E	1068.	995.3	7732.0
1+00E	1072.	1001.7	7732.0
1+20E	1071.	1008.0	7732.0
1+40E	1074.	1014.3	7732.0
1+60E	1079.	1020.6	7732.0
1+80E	1086.	1027.0	7732.0
2B+00E	1090.	1033.3	7732.0
2+00E	1100.	1044.0	7732.0
2+20E	1105.	1050.0	7732.4
2+40E	1109.	1055.9	7732.8
2+60E	1111.	1061.9	7733.2
2+80E	1109.	1067.8	7733.6
3+00E	1108.	1073.8	7734.0
3+20E	1107.	1079.7	7734.4
3+40E	1105.	1085.7	7734.8
3+60E	1104.	1091.6	7735.2
3+80E	1106.	1097.6	7735.6
4C+00E	1112.	1103.5	7736.0
4B+00E	1115.	1109.5	7736.4
4+00E	1113.	1118.0	7737.0
4+20E	1116.	1124.5	7736.9
4+40E	1111.	1130.9	7736.7
4+60E	1107.	1137.4	7736.6
4+80E	1105.	1143.9	7736.5
5+00E	1101.	1150.4	7736.4
5+20E	1100.	1156.8	7736.2
5+40E	1097.	1163.3	7736.1
6+00E	1093.	1170.0	7736.0
6+20E	1096.	1176.2	7736.1
6+40E	1097.	1182.4	7736.2

Station Name	Magnetic Value[1]	UTM Easting[2]	UTM Northing[3]
6+60E	1092.	1188.6	7736.3
6+80E	1086.	1194.8	7736.4
7+00E	1080.	1201.0	7736.5
7+20E	1076.	1207.2	7736.6
7+40E	1072.	1213.4	7736.7
7+60E	1073.	1219.6	7736.8
7+80E	1074.	1225.8	7736.9
8+00E	1073.	1232.0	7737.0

[1]minus 57,000 gammas

[2]minus 350,000

[3]minus 4,920,000 meters